ELSEVIER

Coordination Chemistry Reviews
149 (1996) 125–165

COORDINATION CHEMISTRY REVIEWS

Aluminum and Alzheimer's disease: model studies

Gerald D. Fasman

Graduate Department of Biochemistry, Brandeis University, Waltham, MA 02254, USA

Received 23 January 1995; in revised form 6 April 1995

Contents

Abstract

Model tangles, 13 amino acid sequences and 17 amino acid sequences (NF-M13, NF-M17) have been synthesized and phosphorylated. Circular dichroism studies of their interaction with Ca^{2+} and Al^{3+} have demonstrated the formation of β-pleated sheets. The Ca^{2+} effect can be reversed with citric acid. By the study of synthetic mutants, it has been shown that Al^{3+} binds to COO^-, OH of Ser and the PO_3H of $SerPO_3H$. The β-sheet formation caused by Al^{3+} can be reversed by silicates. βA4 was converted to β-sheets by Al^{3+}, which was also reversed by the addition of silicates. It was suggested that silicates be considered for therapeutic use to delay the onset of plaques and tangles in Alzheimer's disease.

Keywords: Aluminium; Alzheimer's disease

Abbreviations

NFs	neurofilaments
TFE	2,2,2-trifluoroethanol
NF-H	neurofilaments, high M_r
NF-M	neurofilaments, medium M_r
NF-L	neurofilaments, low M_r
NF-M13	Lys-Ser-Pro-Val-Pro-Lys-Ser-Pro-Val-Glu-Glu-Lys-Gly
$(NF\text{-}M13)_3$	NF-M39, trimer of NF-M13
SerP	*O*-phosphorylseryl
NF-M17	Glu-Glu-Lys-Gly-(NF-M13)
CD	circular dichroism
r_{Ca}	$[Ca^{2+}]/[peptide]$
r_{Al}	$[Al^{3+}]/[peptide]$
NF-M17($S^6PS^{11}P$)	NF-M17 with Ser(PO_3H_2) replacing Ser at 6 and 11
NF-M17(A^6A^{11})	NF-M17 with Ala replacing Ser at 6 and 11
NF-M17(A^6)	NF-M17 with Ala replacing Ser at 6
NF-M17($A^6S^{11}P$)	NF-M17(A^6) with Ser (PO_3H_2) replacing Ser at 11
NF-M17(A^{11})	NF-M17 with Ala replacing Ser at 11
NF-M17(S^6PA^{11})	NF-M17(A^{11}) with Ser(PO_3H_2) replacing Ser at 6
NF-M17($A^1A^2A^{14}A^{15}$)	NF-M17 with Ala replacing Glu at each position indicated
NF-M17($A^1A^2A^{14}A^{15}S^6P$)	NF-M17($A^1A^2A^{14}A^{15}$) with Ser(PO_3H_2) replacing Ser at 6
NF-M17($A^1A^2A^{14}A^{15}S^{11}P$)	NF-M17($A^1A^2A^{14}A^{15}$) with Ser(PO_3H_2) replacing Ser at 11
NF-M17($A^1A^2A^{14}A^{15}S^6PS^{11}P$)	NF-M17($A^1A^2A^{14}A^{15}$) with Ser(PO_3H_2) replacing Ser at 6 and 11
NF-M17($A^1A^2A^{11}A^{14}A^{15}$)	NF-M17($A^1A^2A^{11}A^{14}A^{15}$) with Ala replacing Ser at 11
NF-M17($A^1A^2A^6A^{14}A^{15}$)	NF-M17($A^1A^2A^{14}A^{15}$) with Ala replacing Ser at 6
I	initial conformation
β	β-pleated-sheet dominated conformation
M	mixture of conformers or conformational regions
R	random (aperiodic or unordered) dominated conformation
M(R) and M(β)	spectra reflect shifts to the random or β-conformation
M(I)	small conformational change

PPII	poly-L-proline II
$[\theta]_M$	is given in deg cm^{-2} $dmol^{-1}$

1. Introduction

Alzheimer's disease (AD) will probably become the predominant social-medical-economic problem in the next century. An estimated 4 million Americans now have the disease, and this number is expected to grow to >10 million within the next decade [1]. The cause of AD is not known, and treatments are only mildly effective at slowing the degeneration process [2]. The signs of AD, obtained upon autopsy of the diseased brain, reveal two phenomena: amyloid plaques and neurofibrillary tangles [3]. The amyloid plaques are composed primarily of 39- to 42-amino acid fragment (βA4) from the amyloid precursor protein [4]. Tangles contain abnormally phosphorylated tau proteins that combine to form paired helical filaments within the neuron [5]. In addition to the protein components of plaques and tangles, some researchers have detected aluminum [6,7] and aluminosilicates [8] in these lesions, although the evidence for their presence is apparently controversial [9].

Aluminum has been recognized to be a neurotoxic agent, but its etiologic role in Alzheimer disease and other neurodegenerative diseases is still controversial [10–13]. There is debate as to whether plaques precede tangles or vice versa. On the basis of a variety of physiological effects of Al^{3+} in culture and animal systems and its consistent occurrence in neurofibrillary tangles [7,13] and perhaps plaques [13,14], it has been proposed that aluminum is a major risk factor in many neuronal dysfunctions. Others have questioned the etiologic significance of aluminum, mainly because of the failure of some researchers to find it in amyloid plaques by highly sensitive analytic techniques; i.e., laser microprobe mass analysis [15] and nuclear microscopy [8].

There are several ways that enhanced aluminum levels may influence the structural or functional proteinous constituents of nerve cells. The neurotoxicity of aluminum may originate in promoting aggregation of phosphorylated neurofilament subunits, as shown by Díaz-Nido and Avila [16], or catalyzing phosphorylation, or inhibiting dephosphorylation of the tau protein, the main constituent of neurofibrillary tangles (for a survey of the literature; see Refs. [13,17,10]. Nixon et al. [19] and Shea et al. [20] demonstrated that aluminum caused inhibition of proteolysis of neurofilaments in cytoskeletal preparations. Leterrier et al. [21] reported specific interactions with phosphorylated subunits of neurofilaments causing bundling by Al^{3+} and offered a hypothesis for molecular mechanisms of both intra- and interchain interactions.

Aluminum is the third most abundant element in the earth's crust, found primarily as insoluble aluminosilicates and oxides. However, it is soluble as aluminum hydroxide and aluminum hydrates at acidic pH values [22]. This has become a biologic concern as the world's water supplies become more acidic due to acid rain. For example, Birchall et al. [23] have shown that in acidic water (pH 5), aluminum causes damage to gill epithelia and ultimate death for fish. The toxic effect of

aluminum is diminished in the presence of silicic acid as the result of forming hydroxyaluminosilicates.

Silicon is the second most abundant element in the earth's crust and is present in rocks and minerals as SiO_2. It is soluble as $Si(OH)_4$. Implicated as a biologically important element, silicon has been shown in nutrition studies to be vital for growth and development [24]. It has been detected in various human tissues. Silicon provides other beneficial effects in the form of silicic acid as it binds to aluminum [25]; in addition to the results of Birchall et al. [23] mentioned above, silicon has been shown to reduce aluminum accretion in rat brains [26].

This chapter will review the research effort of a collaborative project between two laboratories, Professor M. Hollosi, Eötvös University Budapest and the author. The object of these studies has been to identify regions of "normal" (non-phosphorylated) proteins that could be involved in aggregate formation through conformational changes in the natural sequences or in abnormally phosphorylated analogues thereof. By synthesis of analogues, removing Glu, Ser or SerP sequentially and replacing them with Ala, the sites of binding for metal ions have been determined. These results give insight into the most probable effect of metal ions, mainly Al^{3+} and Ca^{2+}, on their binding to "model tangle" sequences and to βA4 (A-42) and causing β-sheet conformations in both.

2. NF-M initial studies

The proteins found in tangles in neurons have been classified according to size: NF-H (neurofilament-heavy, 210 kDa) NF-M (Neurofilment-medium, 160 kDa) and NF-L (neurofilament-light, 70 kDa). We have chosen NF-M as our target protein. As a 13 amino acid sequence is repeated six times contiguously in NF-M, we synthesized this as a model.

The biological significance of the phosphorylated NF-M13 has been described by Lee and coworkers [27,28]. The NF-M13 peptide, its dimer and trimer were synthesized [58] as well as their phosphorylated species (Table 1). The secondary structure was analyzed by circular dichroism spectroscopy, secondary structure prediction and conformational energy calculations.

Both the phosphorylated and nonphosphorylated fragments of NF-M13 and NF-17 of the human neurofilament protein are conformationally mobile systems (NF-M17 has the tetra peptide on the carboxyl terminal of NF-M13, attached again to the amino terminal). They display three different types of CD spectra (Fig. 1). In water (pH 6), all peptides (except NF-M13P) exhibit spectra typical of those of the unordered or random coil structure [30]. Changes of pH in the 2–12 range had no effect on the CD curves.

Forces between H_2O-solvated NH_{3+} and $PO_3H_2^-$ groups are presumably not strong enough to alter the "unordered" conformation of the parent peptide. The rationale for using trifluoroethanol (TFE) was to stimulate the low dielectric constant of the neuron, or the brain in general. In TFE the trimer $(NF\text{-}M13)_3$ and NF-M13 show a CD spectrum similar to that of an α-helix [30] except the band intensities

Table 1
Circular dichroism spectra, in trifluoroethanol, of NF-M fragments and phosphorylated NF-M (P) fragments [42]

Sequence	Abbreviation	$n\pi^*$		$\pi\pi^*$ bands			
		λ (nm)	$[\theta]_M$	λ (nm)	$[\theta]_M$	λ (nm)	$[\theta]_M$
2 7 13 K S P V P K S P V G E K G	NF-M13	218.5	(−6400)	204.5	(−8500)	~187	(8100)
— S — PO_3H_2	NF-M13 Ser^2P	~221br[a]	(−6500)	205	(−8800)	~196	(6400)
— S — PO_3H_2	NF-M13 Ser^7P	~222	(−4000)	205	(−4400)	~191	(3750)
−4 −1 2 7 13 E E K G K S P V P K S P V E E K G	NF-M17[d]	220.5	(−7294)	205	(10510)	189	(6848)
— S — PO_3H_2	NF-M17 Ser^2P[c]	222.5	(−6050)	208	(−6550)	~190	(8350)
— S — PO_3H_2	NF-M17 Ser^7P[c]	~220	(−5200)	207.5	(−5500)	~189	(5700)
7 P K S P V - NH_2 PO_3H_2	NF-M5-NH_2Ser^7P	219	(−3550)	201	(−5100)	<190	(max)
7 Ac- P K S P V - NH_2 PO_3H_2	Ac-NF-M5-NH_2Ser^7P	~215sh[b]		203	(−8650)	<190	(+max)

TFE, trifluoroethanol. [a] br, broad; [b] sh, shoulder; [c] amide at the C-terminus.

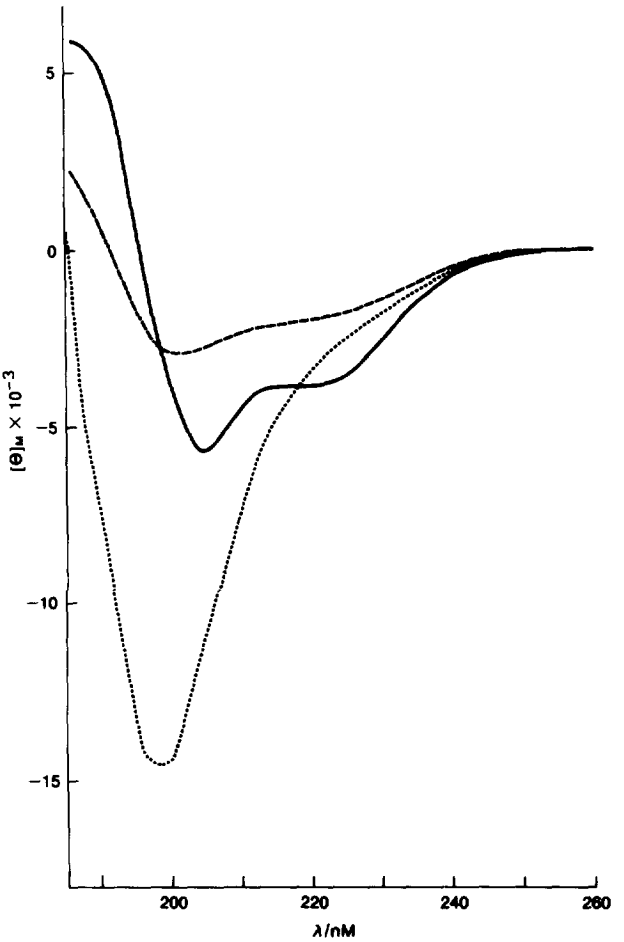

Fig. 1. Circular dichroism spectrum of peptide 1–39 in TFE (—) and water (····) and that of peptide 1–39 in TFE (- - - -). Concentrations of peptides ranged from 0.4 to 1.0 mg ml^{-1}. Mean residue ellipticity, $[\theta]_M$, is expressed in deg cm^{-2} $dmol^{-1}$ by using a mean residue weight of 108.7 [58].

are significantly lower than those of α-helices. This CD spectra is similar to that measured for β-turns, with established Type I(III) character [31–34].

Application of the predicative secondary structural algorithm of Chou and Fasman [35] on the non-phosphorylated peptides revealed that both peptides showed a strong tendency to form both β-turns and short segments of α-helix (Fig. 2). Thus, the repeating neurofilament NF-M [36] would have a repeating secondary structure of β-turn, α-helix, β-turn, β-turn, α-helix, β-turn, β-turn, and so forth. It was found that the 13-mer and the 39-mer had the same CD curves in TFE, which indicates that there is no interaction between the ordered portions of the chain of peptide $(NF\text{-}M13)_3$. A β-turn can be regarded as a single turn of a 3_{10} helix [37,38].

The CD curve of peptide $(NF\text{-}M13)_3$ in TFE (Fig. 1) was analyzed by the deconvo-

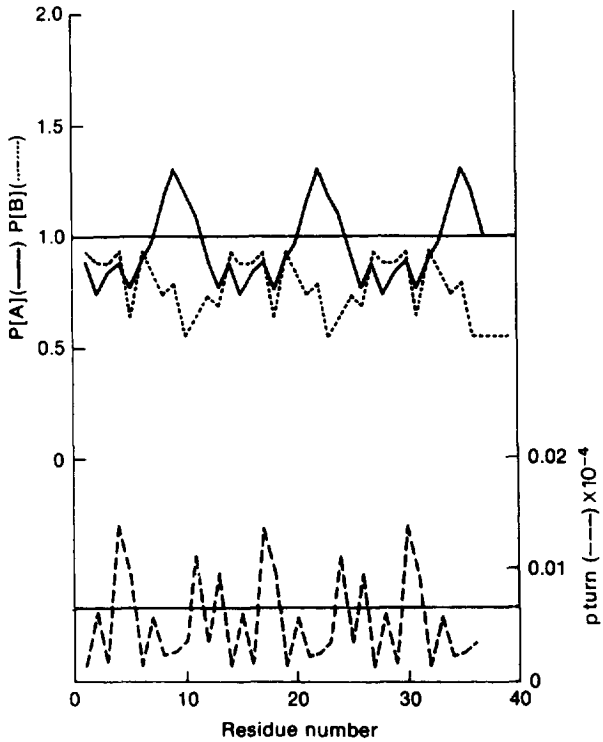

Fig. 2. Computer prediction of the secondary structure (α-helix, β-pleated sheet and β-turn) of peptide 1–39. Values above the threshold limit (horizontal lines) indicate the α-helix and β-turn potential, respectively, of the given segments [58].

lution method (CCA) [39,40] and was found to contain 6.5% α-helix, 45% type I(III) β-turn, 38% type II β-turn and 10.5% unordered structure.

Hard-sphere conformational energy calculations performed on the peptide Ac-Pro^5-Lys-Ser-Pro-Val-Glu-Glu-Lys-Gly^{13}-NHCH$_3$ gave support to the predicted secondary structure obtained by CD.

CD titration studies with Ca^{2+} and Al^{3+} on both non-phosphorylated and phosphorylated peptides corresponding to partial sequences of human NF-M13 and NF-M17 were also undertaken [41]. The rationale for studying both Al^{3+} and Ca^{2+} is predicated on the finding of high Ca^{2+} concentrations in Alzheimer neuronal cells. Thus, Ca^{2+} might bind to these proteins and then be replaced by Al^{3+}.

3. Metal ion-induced conformational changes [42]

Neurofilaments (NFs) are abundant in cytoskeletal structures. NF proteins form filaments, via coiled-coil interactions, between structurally conservative "rod" sequences of the high, medium and low M_r (NF-H, NF-M and NF-L) subunits. In

NF-H and NF-M proteins, long polypeptide sections (400 to 600 residues) follow the homologous rod regions on the C-terminal side [43–45]. It is these regions protruding from the NF backbone that most likely determine the surface properties of NFs, and thus, at the molecular level, their tendency to form aggregates.

The amino acid sequence of human NF-M has been determined [36]. The C-terminal domain was found to contain a 13-mer sequence, Lys-Ser-Pro-Val-Pro-Lys-Ser-Pro-Val-Glu-Glu-Lys-Gly (NF-M13), which was repeated contiguously six times. In this 78-residue block the Lys-Ser-Pro-Val tetramer occurs 12 times. A related Lys-Ser-Pro-Ala tetramer is tandemly repeated many times in the analogous C-terminal domain of rat NF-H [47]. On the basis of circular dichroism (CD) studies [28], the rod region of NF proteins adopts an α-helical conformation, while the C-terminal (tail) domains show CD spectra characteristic of the unordered conformation. According to comparative in vivo and in vitro studies, the N-terminal (head) and C-terminal (tail) domains of NF-M appear to be selectively phosphorylated by separate kinase systems [47]. (For a detailed analysis of the phosphorylation of NF proteins see Sihag and Nixon [48], and the references cited therein.)

The microtubule-associated protein tau can also be phosphorylated by a calcium/calmodulin-dependent kinase [49] and by protein kinase C [49,50]. Its sequence has many potential phosphorylation sites of the type Lys-Ser(Thr)-Pro-X (X = Pro, Ser or Val), and its Lys-Ser-Pro-Val tetramer is identical with the postulated repeating phosphorylation site of NF-M.

The partial sequence of another human NFT protein, MAP2, was elucidated [51]. This protein can be highly phosphorylated by several kinases, including the Ca^{2+}/calmodulin-dependent kinase [52] and the cyclic AMP-dependent kinase [53]. Their phosphorylation sites, the Arg-X-Y-Ser(Thr), Arg-Arg-X-Ser-X and Lys-Arg-X-X-Ser-X peptides, occur may times throughout the sequence of MAP2 [50]. The immunological similarity of the multiphosphorylation repeat of human NF-M with regions of tau and MAP2 [54–57], as well as with neurofibrillary tangles [56,57] suggest sequence and/or structural homologies between the two groups of cytoskeletal proteins.

Phosphorylation is expected to have a marked effect on the conformation of proteins [58]. It was suggested that a periodic conformation of NF-M13 and its trimer, $(NF\text{-}M13)_3$, existed. NF-M13 contains two serine residues per subunit. On the basis of CD studies on hyperphosphorylated derivatives of NF-M13 and NF-M39, phosphorylated derivatives of NF-M13 and NF-M39, phosphorylation was found to destroy this periodic structure.

Fig. 3. (a) Circular dichroism (CD) titration of NF-M17 Ser^2P in TFE with Ca^{2+} ions. [pep] = 8.4×10^{-5} mol l^{-1}. 1, no Ca^{2+}; $[Ca^{2+}]/[pep]$ ratios for line 2, 2; line 3, 10; line 4, 20. CD titration experiments were performed in a 0.05 cm cell. CD spectra were taken at 10–20 different [metal]/[peptide] ratios. The concentration of the stock solutions was based on quantitative amino acid analysis. $Ca(ClO_4)_2 \times H_2O$, 22.2% H_2O (Alfa) and $Al(ClO_4)_3 \cdot 9H_2O$ (Aldrich) were used. Data were evaluated by a CD curve deconvolution algorithm (convex constraint method) [42]. (b) Circular dichroism titration of NF-M17 Ser^2P in TFE with Al^{3+} ions. [pep] = 8.4×10^{-5} mol l^{-1}. 1, no Al^{3+}; $[Al^{3+}]/[pep]$ ratios for line 2, 2; line 3, 5; line 4, 10 [42].

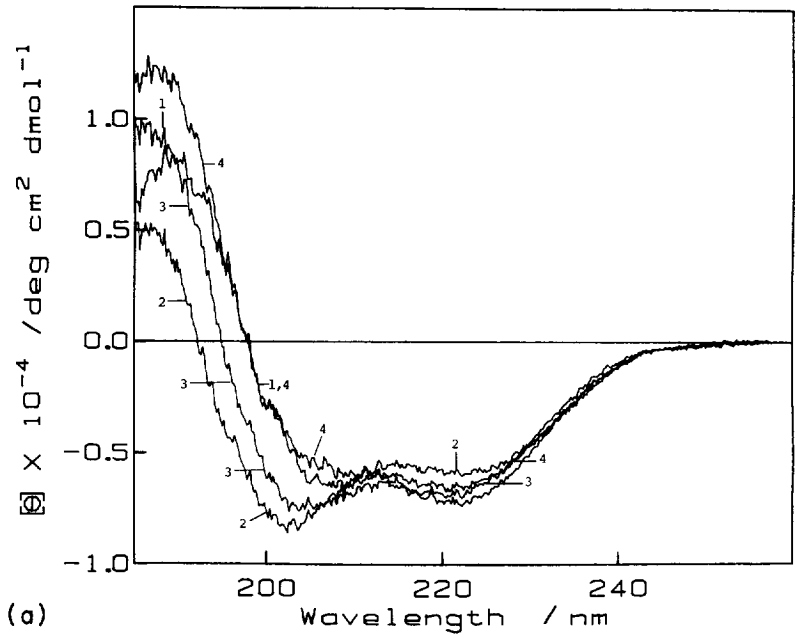
[Θ] X 10⁻⁴ /deg cm² dmol⁻¹
1.0
0.5
0.0
−0.5
−1.0
200
220
240
Wavelength / nm
(a)

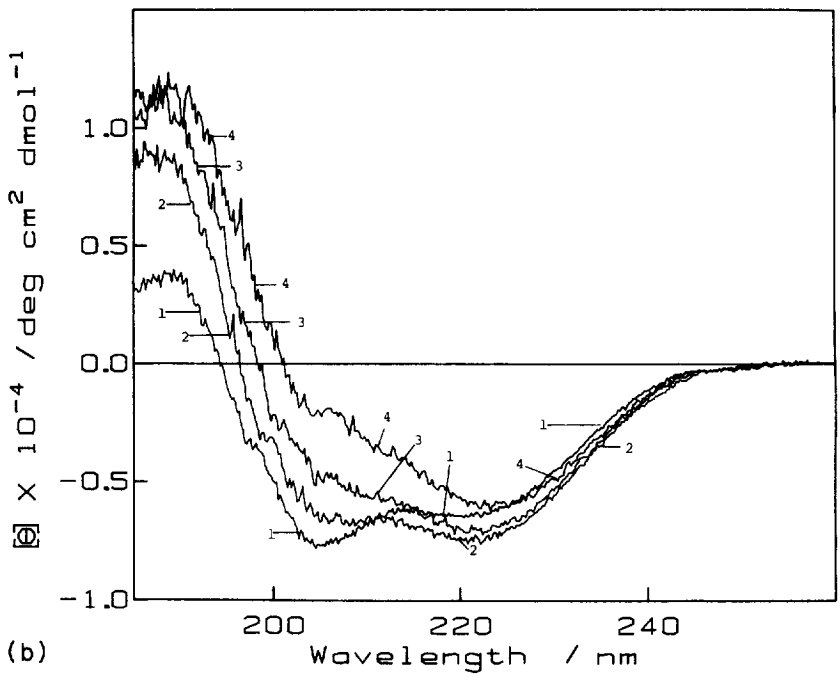
[Θ] X 10⁻⁴ /deg cm² dmol⁻¹
1.0
0.5
0.0
−0.5
−1.0
200
220
240
Wavelength / nm
(b)

Peptides containing *O*-phosphorylated seryl or threonyl residue(s) have an expressed tendency to bind alkaline earth metal ions [59]. Two neighboring *O*-phosphoryl [60] or glutamate [61] groups can form chelates with multi-valent metal ions and an *O*-phosphoryl residue with a vicinal carboxylate or a hydroxyl containing side-chains may also have a chelating effect. A critical survey of the crucial role of Ca^{2+} and Al^{3+} in ageing brain and neurodegenerative diseases is given in several reviews (e.g. see Khachaturian [10]).

The study of the site-specific conformational effect of phosphorylation and metal ion binding requires selectively phosphorylated peptides. Reverse-phase high pressure liquid chromatography (HPLC) separation of synthetic phospho-peptide isomers [62] yielded NF-M fragments containing an *O*-phosphoseryl (SerP) residue at different positions (Table 1).

Ca^{2+} and Al^{3+} titrations of phosphorylated NF-M17 fragments, measured in TFE, showed remarkable changes in the CD spectra (Fig. 3(a,b)). The deconvolution [39,40] of the CD titration curves of NF-M Ser^2P indicates an increase of the unordered structure component at low Ca^{2+} excess (75% at ratio 2), and at high Ca^{2+} excesses a decrease of the unordered structure component and a simultaneous gradual increase of the β-pleated sheet component ($\sim$55% unordered structure and $\sim$45% β-pleated sheet at ratio 30).

The CD titration curves of NF-M17 Ser^7P with Ca^{2+} yield similar results to those found with Al^{3+}; however, they show significant differences (Fig. 4(a,b). Upon Ca^{2+} titration, the unordered structural component increased slightly before decreasing while the Al^{3+} titration did not exhibit this initial decrease. With the diphospho derivative, NF-M17 Ser^2PSer^7P, Ca^{2+} titration first caused the appearance of more of the unordered structure component of the CD curves, as found with the monophosphates. However, at high concentrations of Ca^{2+} ($[Ca^{2+}]/[pep] > 3$), a gradual increase in the amount of the β-pleated sheet spectrum was observed, peaking at a ratio of $\sim$0. Further increases in Ca^{2+} concentration causes precipitation. Al^{3+} titration of the diphospho derivative, NF-M17 Ser^2PSer^7P shows a continuous increase in the β-pleated sheet component spectrum. The maximum is reached at $[Al^{3+}]/[pep] \sim 7.5$.

CD spectra of aqueous solutions of Ser^2P, Ser^7P and Ser^2PSer^7P derivatives of NF-M17 all yielded a negative band below 200 nm, indicating the unordered conformation [37,64]. These spectra do not change upon the addition of metal ions up to ratios of [metal ions]/[pep] $\sim$ 30. Metal ion binding cannot be excluded even in aqueous solution; however, it is not effective enough to change the backbone conformation of the highly solvated phosphopeptides.

TFE is well known to have a helix-promoting effect [65]. On the basis of high-resolution NMR experiments [66], TFE appears to stabilize incipient structures previously detected in aqueous solution. CD titration curves measured in TFE can be deconvoluted into two spectral components. Allowing for a contribution of a third subspectrum (3-component deconvolution) did not result in a significant decrease of the error of the deconvolution. This suggests that the secondary structure of phosphorylated NF-M fragments is composed of two major components having differing chiropractical contributions. CD spectra marked by a strong negative band

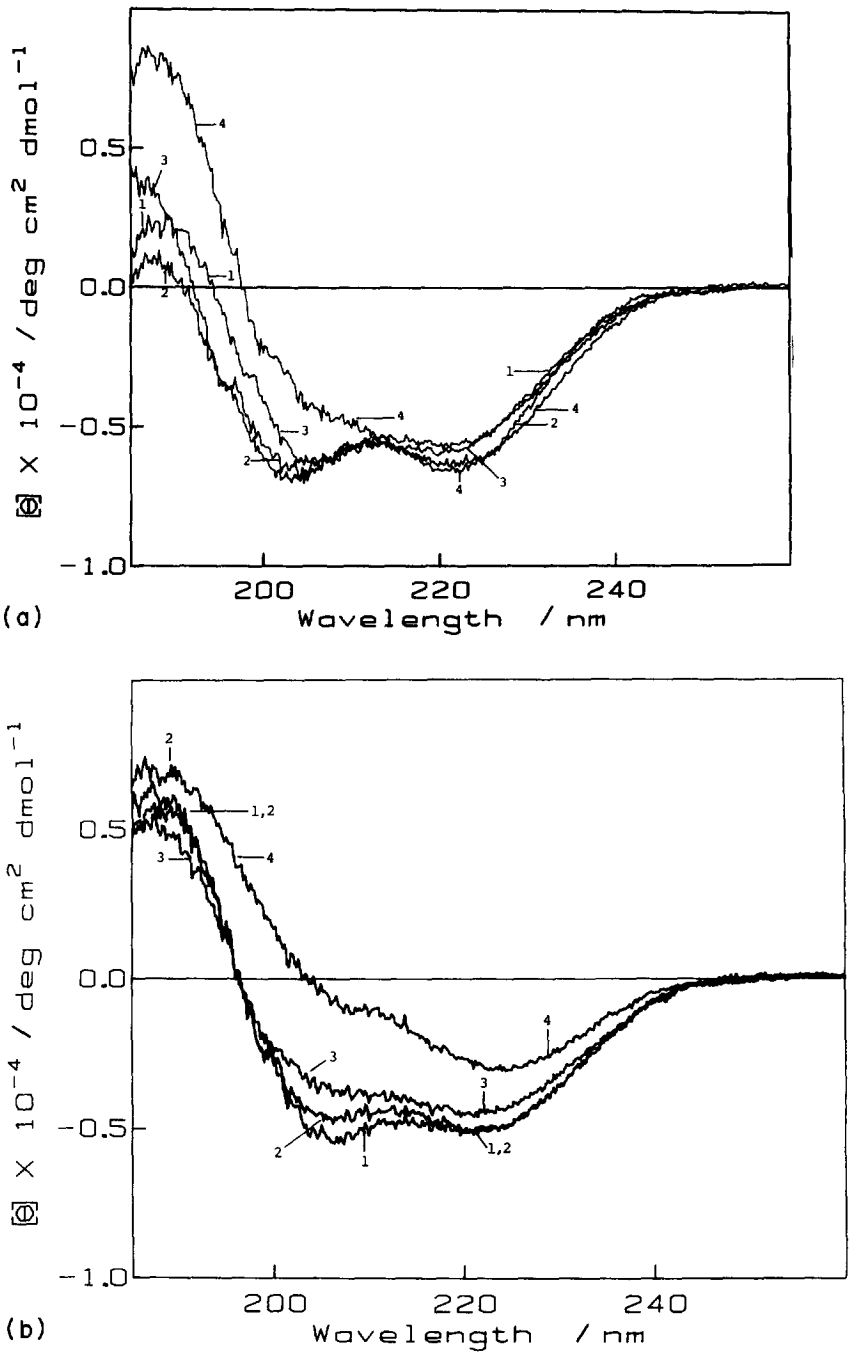

Fig. 4. (a) Circular dichroism titration of NF-M17 Ser^{7}P in TFE with Ca^{2+} ions. [pep] = 1.2×10^{-4} mol l^{-1}. 1, no Ca^{2+}; [Ca^{2+}]/[pep] ratios for line 2, 1; line 3, 5; line 4, 15 [42]. (b) Circular dichroism titration of NF-M17 Ser^{7}P in TFE with Al^{3+} ions. [pep] = 1.2×10^{-4} mol l^{-1}. 1, no Al^{3+}; [Al^{3+}]/[pep] ratios for line 2, 1; line 3, 5; line 4, 10 [42].

near 200 nm are generally expected to reflect the presence of an unordered (or aperiodic) conformation of peptides [37,65]. However, considering the unexpected red shift [67] of the negative bands of unordered structure spectra in TFE (Figs. 3(a) and 4(a)), it is reasonable to suppose that a portion of the peptide sequence adopts a poly-L-proline II (PPII) [68–70] conformation instead of an aperiodic one. The intermediate (Ser-Pro-Val-Pro-Lys-Ser-Pro-Val) segment of NF-M17 contains three proline residues. Serine also has a high probability of adopting a PPII conformation [71,72]. An X-ray analysis [71] of the avian pancreatic polypeptide, at 0.98 Å resolution, showed that residues 2 to 8 (Pro-Ser-Gln-Pro-Thr-Tyr-Pro) adopt a PPII conformation with mean torsion angles $\theta = -72°$, $\psi = 140°$, The CD spectrum of a PPII shows a strong negative extremum near 206 nm and a weak positive one above 225 nm [68–70]. In the spectra reported here the positive band is obliterated by the stronger negative CD band above 220 nm, of the other β-pleated sheet spectral component.

On the basis of its spectral parameters, the deconvoluted CD curve can be assigned to segment(s) adopting extended or β-pleated sheet-like conformation. The predominant CD feature of β-pleated sheet structures is the appearance of a negative band near 216 nm and a positive band between 195 and 200 nm [37,64].

To discriminate between the conformational effects of binding metal ions to the two glutamic acid residues at positions 10 and 11 in NF-M13 from binding to the serine-phosphate (Ser^2P or Ser^7P) sites, CD titrations with Ca^{2+} were carried out on shorter phosphorylated fragments: Pro-Lys-SerP-Pro-Val-NH_2, *N*-acetyl-Pro-Lys-SerP-Pro-Val-NH_2, and non-phosphorylated NF-M13. The first two listed peptides contain a serine-phosphate, while NF-M13 contains a C-terminal Glu-Glu binding site. The pentapeptide fragments Pro-Lys-SerP-Pro-Val-NH_2 and *N*-acetyl-Pro-Lys-SerP-Pro-Val-NH_2 yielded unordered structure type CD spectra (Table 1) in TFE, which did not change on addition of ten equivalents of Ca^{2+}.

Complexing of Ca^{2+} resulted in a marked change in the CD spectra of all three phosphorylated fragments of NF-M17 in TFE. The conformation shifts from an unordered (or poly-L-proline II) structure to one that has a high β-pleated sheet content. There is, however, an important difference in the Ca^{2+} dependence of the spectra of these fragments. Titration curves (Figs. 3(a) and 4(a)) and deconvolution data indicate that phosphorylation at Ser^2 initially delays the conformational change giving rise to the β-pleated sheet spectra. Moreover, at high Ca^{2+} excess the amount of β-pleated sheet component is much lower for NF-M17 Ser^2P than for its Ser^7P isomer. The spectra of NF-M17 Ser^2PSer^7P show an intermediate Ca^{2+} sensitivity.

On the basis on the CD titration data, Ca^{2+} and Al^{3+} binding by phosphorylated NF-M17 fragments is accompanied by the adoption of an extended or β-pleated sheet conformation above a critical level of the metal ion concentration, which also depends on the position of the phosphoserine residue (Ser^2 or Ser^7). Al^{3+} binding brings about a direct increase of the β-pleated sheet conformation and the predominance of this conformation is reached at lower concentrations than in the case of Ca^{2+} binding. The β-pleated sheets so formed precipitate on standing. A hypothesis for the mechanism of β-pleated sheet formation is the following: the metal ions bind to phosphates or carboxylates on one polypeptide fragment, neutralizing the negative

charge, and then cross-link, in the same fashion, to a second fragment. This causes chain association which produces the β-pleated sheet conformation, a highly insoluble structure.

The main difference between the Ca^{2+} and Al^{3+} induced backbone extension process of phosphorylated NF-M17 fragments is that low Ca^{2+} concentrations first cause a decrease in the amount of the extended (β-pleated sheet) conformation. The gradual increase of the β-content occurs only above a critical [Ca^{2+}] level which depends on the site and number of phosphoryl group(s) in the molecule (Figs. 3(a) and 4(a)). In the presence of Al^{3+}, a rather steep increase of the β-content can be observed for all three phosphorylated fragments (Figs. 3(b), 4(b)). The difference in the conformational effect of Ca^{2+} and Al^{3+} complexing may be accounted for by the enhanced Al^{3+} binding affinity of the glutamate (and presumably) phosphate site(s) and by the differing geometric and thermodynamic conditions of trivalent metal ion complexing [73].

On the basis of the CD evidence, the following model is proposed for the backbone extension to form β-pleated sheets of the repeating domain of NF-M protein (Fig. 5). Phosphorylation in the natural position (Ser^2) stabilizes a PPII-like conformation (Fig. 5, route A). Moreover, the phosphoserine residue may act as an internal Ca^{2+} storage site. By binding Ca^{2+}, it buffers fluctuations of the Ca^{2+} concentration and delays Ca^{2+} binding to the glutamate site, which is most likely responsible for the PPII β-pleated sheet conformational change. Abnormal (Ser^7) and hyperphosphorylation (Fig. 5, route B) of the peptide, by decreasing the stability of the central PPII structure, results in higher β-pleated sheet content (65 to 70%) and an expressed sensitivity towards Ca^{2+} ions. Thus, a small increase of the Ca^{2+} concentration can give rise to a predominantly β-pleated sheet conformation of the repeating domain. As pointed out earlier, aluminum is a more potent β-pleated sheet inducer. While a 10-times molar excess of Ca^{2+} induces only a 30% β-pleated sheet conformation in the Ser^2P fragment, 3 equivalences of Al^{3+} increases the β-content to 70%. In abnormally (Ser^7) phosphorylated and hyperphosphorylated fragments a relatively small Al^{3+} excess leads to a prevailing β-pleated sheet structure.

Experiments have indicated that no high-affinity Ca^{2+}-binding sites were found in the soluble C-terminal domains of NF-H and NF-M [59]. However, phosphoserine residues located in the C-terminal domains of NF subunits appear to have a regulatory effect on the accessibility of the high-affinity Ca^{2+}-binding sites in the N-terminal core region. It was also shown that Al^{3+} binds not only to the high- but also to the low-affinity binding sites on NFs. In Al^{3+}-induced neuropathies, the NFs of neuronal perikarya of animals injected with Al^{3+} are in a hyperphosphorylated state [73]. Aluminum salts cause argyrophilic accumulations in perikarya of many NB2a(−) and NB2a(+) neuroblastoma cells [74]. The Al^{3+}-induced direct PPII→β-pleated sheet conformational change of Ser^7P and Ser^2PSer^7P hyperphosphorylated NF-M fragments, reported herein, strongly suggests that it is the C-terminal part of NF proteins which is involved in early stages of the aggregation.

An attempt will be made to correlate the results reported herein with observations relative to Alzheimer's and related diseases. The common feature of these neurodegenerative diseases is the accumulations of fibrous proteinaceous structures such as

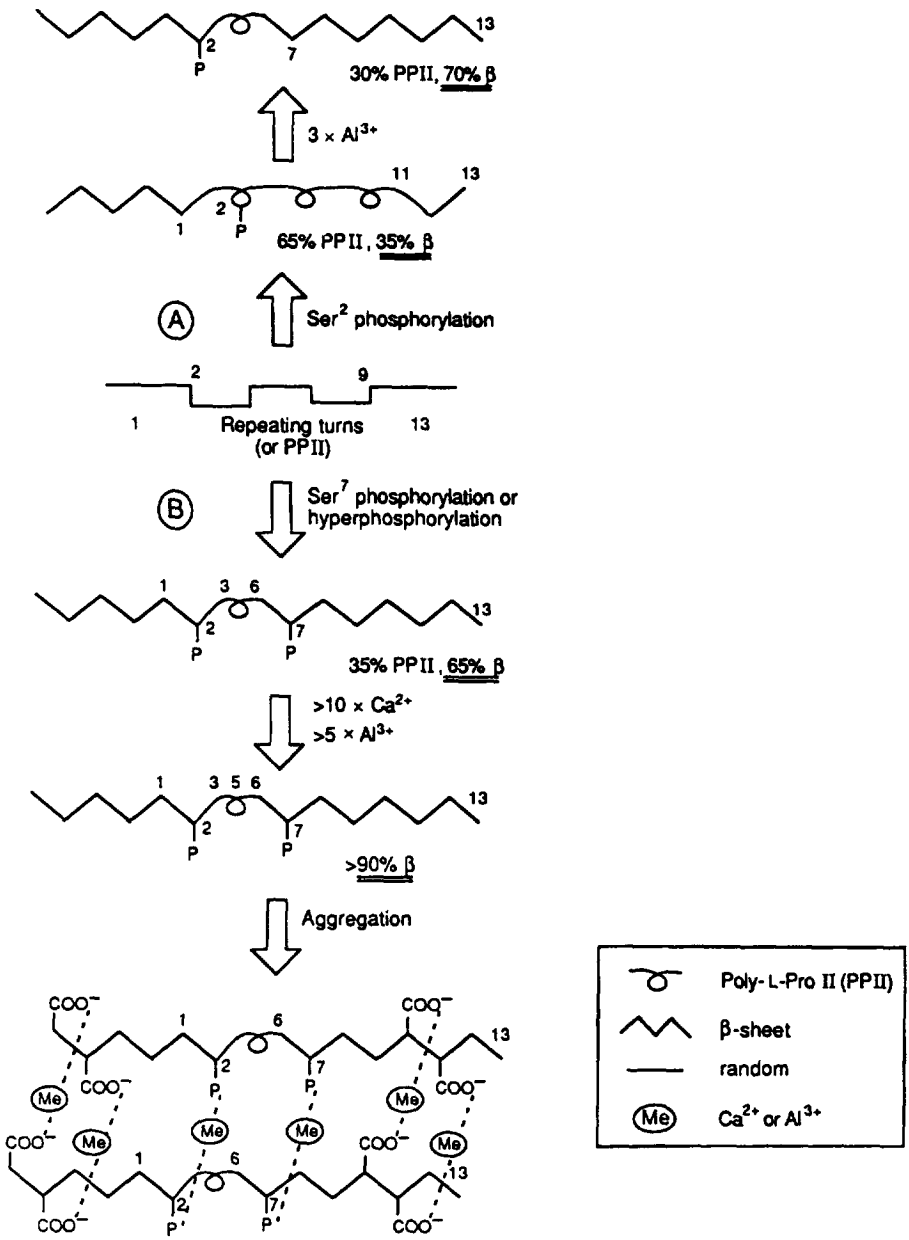

Fig. 5. Proposed mechanism of metal ion induced β-pleated sheet formation of the C-terminal repeating domain of phosphorylated NF-M protein. Route A: retarding effect of Ser^2 (normal) phosphorylation; Route B: β-pleated sheet inducing effect of Ser^7 (abnormal). β-pleated sheet formation of hyperphosphorylation [Ser^2PSerP^7P] and the PPII$\rightarrow\beta$ transition induced by metal ions [42].

neurofibrillary tangles (NFT) and senile plaques [75]. These NFTs contain NF proteins as well as other components [27]. These tangles are organized in a cross-β-pleated sheet structure, although none of the components of NFTs are predicted to assume the β-sheet conformation [43–45,76]. It has been suggested that an imbalance within specific kinases responsible for the phosphorylation of different sites in neurofilaments may be involved in the formation of Alzheimer's lesions [77]. The selected sequences of the NF-M which were synthesized and studied (Table 1) allowed the investigation of the role of phosphorylation at two different sites (Ser^2 and Ser^7). Aberrant phosphorylation of the NF-M protein may lead to an increasing number of SerP residues in the Ser^7 position, thus causing their aggregation.

A recent electron microscopic study [78] shows that the accumulation of neurofilaments may be caused by abnormal levels of multivalent cations. However, there is a wide variation in the level of the effective cation concentration (0.1 mM for Gd^{3+}, 0.75 mM for Al^{3+}, 10 mM for Ca^{2+} and 30 mM for Mg^{2+}) [78]. It has also been observed that some neurofilament proteins become less soluble in the presence of Ca^{2+} ions [79]. These findings agree with the results herein and can be satisfactorily explained by the increased affinity of trivalent cations towards binding sites, whose saturation triggers backbone β-pleated sheet formation and chain association. Multivalent metal ion binding may play a role not only in the backbone extension (or backbone β-pleated sheet formation) but also in promoting aggregation of neighboring β-chains by binding to the carboxylate and phosphate side chain groups and shielding their repulsion. Cytoskeletal proteins of nerve cells probably consist of large α-helical [44] and poly(L-proline) II-like conformational domains.

Associations of β-pleated sheet chains due to conformation-sensitive monophosphorylation or hyperphosphorylation and with subsequent Ca^{2+} or Al^{3+} binding may serve as cores for progressive aggregation of NF proteins or the cross-aggregation of NF and microtubule-associated proteins characteristic of neurofibrillary tangles. The Al^{3+} concentration used herein (0.1 mM to 1.0 mM) to produce the observed conformational changes may not accurately reflect the concentrations of free Al^{3+} ions in solution. As pointed out [19], the concentration of free Al^{3+} ions in specific cells is uncertain because of ion selective permeability and specific binding to proteins, and may be higher than that reported for the whole tissue. The concentration of Al^{3+} in a degenerating cell [81], where the selectivity has been altered, may be higher than in the normal cell. By activating kinases or phosphatases, multivalent metal ions may also play a crucial role in determining the phosphorylation state of NF-M and microtubule-associated proteins. Thus, multivalent cations may affect the process of aggregation in a two-fold manner. The model suggested in Fig. 5 gives a possible explanation for both the complexity of the tangle-inducing aggregation process and the differing roles that Ca^{2+} and Al^{3+} ions are likely to play in it. Although the model suggests that abnormal or hyper-phosphorylation is necessary to cause aggregation, it is also feasible that normal phosphorylated NF proteins may aggregate if the Ca^{2+} or Al^{3+} concentration is increased in the cell. The observations discussed herein may have relevance to the mechanism of tangle formation associated with Alzheimer's disease.

4. Stable intrachain and interchain complexes [80]

CD spectroscopic studies on two synthetic fragments of human neurofilament protein mid-sized subunit (NF-M), NF-M13 (KSPVPKSPVEEKG) and NF-M17 (EEKGKSPVPkSPVEEKG), and their alanine-substituted and/or serine-phosphorylated derivatives were carried out in an attempt to find a molecular mechanism for the effect of Al^{3+} to induce aggregation of neuronal proteins of their catabolic fragments. Al^{3+} and Ca^{2+} ions were found to induce β-pleated sheet formation in the phosphorylated fragments. The cation sensitivity depended on the length and charge distribution of the sequence and site of phosphorylation. Al^{3+}-induced conformational changes were irreversible to citric acid chelation, whereas Ca^{2+}-induced conformational changes were reversible with citric acid. Studies of the alanine derivatives demonstrated which residues affected Al^{3+} or Ca^{2+} binding. Peptides containing at least one free (nonphosphorylated) serine residue were shown to form an intramolecular Al^{3+} complex, rather than an intermolecular one. In the intramolecular (intrachain) complex, the ligand function of the deprotonated serine hydroxyl was delineated [(Al·pepH$_{-1}$)-type complex]. Ca^{2+} ions did not show a tendency for intramolecular complexing. The potential role of Al^{3+} in Alzheimer disease tangle and plaque formation is strongly suggested.

The cation sensitivity depended on the length and charge distribution of the sequence and the site and degree of phosphorylation. A β-sheet inducing effect of both cations was generally observed in the case of the serine-phosphorylated fragments (Fig. 6(B)). However, addition of increasing amounts of Al^{3+} ions to the trifluoroethanol (TFE) solution of the parent (nonphosphorylated) peptides, NF-M13 or NF-M17, containing a free serine(s) in the C-terminal [7 or 11] position, or both positions, failed to give rise to CD spectral changes reflecting chain extension and β-sheet formation. The CD titration studies clearly indicated that the Al^{3+}-induced conformational changes, regardless of whether they were characteristic of the β-sheet conformation or not, are practically irreversible in TFE; that is, they cannot be reversed by citric acid, a high affinity chelator of Al^{3+} ions [81]. Contrary to this, the Ca^{2+}-induced spectral transitions proved to be reversible; i.e., they could be reversed by citric acid in all cases.

CD-monitored cation binding studies on the alanine-substituted derivatives [82] have indicated that neurofilament peptides, having a free (nonphosphorylated) C-terminal, or two serine residues, bind Al^{3+} irreversibly, but the spectral change is

Fig. 6. (A) Hypothetical model of the C-terminal-type [Al·pepH$_{-1}$]$^-$ complex of NF-M17. One of the three carboxylates is unbound or weakly bound. The semicyclic structure may also be stabilized by a salt-bridge. The model is based on studies on the [Al·cit$_{-1}$]$^-$ complex, where one of the three carboxylates is unbound or only weakly bound. (B) Hypothetical model of the C-terminal [Al^n·L$_2$] type aluminum polycomplex of [Ser^{11}P]NF-M17. The β-strands are crosslinked by Al^{3+} bridges above and below the plane of the sheet. Salt bridges may also be effective in connecting the neighboring chains (not shown). Al^{3+} bridges are also formed at the N terminus, whereas the central part of the molecule does not take part in β-pleated sheet formation. (C) Possible routes of Al^{3+}-induced tangle and plaques formation. NF, neurofilament [80].

A **Intrachain Complexing**

$[Al \cdot pepH_{-1}]$ =

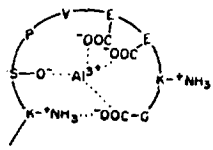

B **Interchain Complexing**

$[Al^{n}L_{2}]$ =

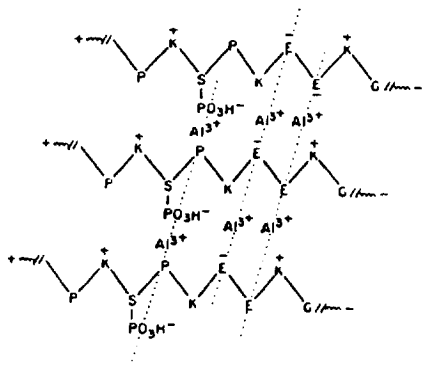

C **Hypothetical Model of the C-terminal Type**

$[Al \cdot lH_{-1}]^{-}$ Aluminum Complex

$[Al \cdot pepH_{-1}] \rightleftarrows [Al^{n} \cdot L_{2}] \rightleftarrows [Al^{mn}\ L_{m}]$

↓ ↓

enzymatic or chemical catalysis of the phosphorylation of cytoskeletal proteins

extensive aggregation (possible formation of co-aggregates)

↙ ↘ Al, Ca^{2+} ↓

aggregation (tau ?) aggregation (NF protein) tangle (plaque ?) formation

↓

tangle formation

not characteristic of a shift of the conformational equilibrium towards β-sheets. A clear cut β-sheet shift was observed for Al^{3+} only in the case of NF-M17(A^6A^{11}), having no free serine residues. By contrast, Ca^{2+} ions yielded a CD spectrum with a higher β-sheet content only if both serines were present in the molecule. Any Ca^{2+}-induced spectral changes could be reversed by citric acid. NF-M17($A^1A^2A^{14}A^{15}$), with all glutamates substituted by alanines, also showed a definite spectral shift toward the β-conformation, but only upon addition of Ca^{2+} ions [82]. It was the coordination chemistry of aluminum that provided an explanation for the surprising selectivity toward the ligand groups of neurofilament peptides. Citric acid is an excellent chelator of Al^{3+} (log $K = 8.1$ near 0.15 M ionic strength at 25 °C) [81,83]. It forms a less stable complex with Ca^{2+} (log $K = 3.5$ at 0.15 M ionic strength [84] or 3.15 at pH = 9.15 in 0.1 M $Na_2B_4O_7$ buffer, and 2.85 in the same buffer at pH = 7.3 in the same buffer, pH adjusted with conc. HCl) [82]. The OH group of citric acid has a central role in Al^{3+}-binding. At $3 < pH < 8$ values, the predominant complex species is $[Al{\cdot}citH_{-1}]^-$ in which the citrate ion serves as a tridentate ligand with two carboxylates and a deprotonated OH group [81,83]. Indeed, citrate forms a 270-times stronger complex with Al^{3+} than does 3-carboxy-1,5-pentane-dioate (citrate lacking the 3-hydroxy group) [83]. In this complex the oxygens of the deprotonated citrate (hydroxy group) act as bridges for the other Al^{3+} ions. The ligand function of the hydroxy group is also verified by X-ray crystallographic [85] data on the glycolate [84,86] and lactate [86a] complexes of Al^{3+}. The crystal structure of a stable trinuclear Al^{3+}-citrate complex, $[Al_3(H_{-1}cit)_3(OH)(H_2O)]^{4-}$, has been reported [87]. In this complex the oxygens of the deprotonated citrate hydroxy groups act as bridges for the other Al atoms. Clearly, the hydroxy oxygen is superior to that of carboxylate as a ligand of Al, but the most stable Al^{3+}-complexes are formed with the participation of both the hydroxy and carboxylate oxygens.

The coordination space of Al^{3+} is more flexible than that of Ca^{2+} [83]. The coordination chemistry of Al^{3+} is closer to Mg^{2+} than that of Ca^{2+} [85]. This explains the high affinity of Al^{3+} to ATP [88]. CD-monitored Al^{3+} titration data on the alanine-substituted NF-M fragments have shown that one hydroxy and one or more carboxylate groups attached to a peptide chain in the proper sequential order may also form type $[Al{\cdot}citH_{-1}]^-$ complexes. In these intrachain complexes (Fig. 6(A)), the peptide molecule is folded in such a fashion that it prevents the adoption of the β-sheet conformation. In the other interchain type of complexes, the ligand groups of Al^{3+} come from different peptide chains (Fig. 6(B). This implies that Al^{3+}-bridges are formed which link neighboring peptide chains. The Al^{3+}-bridges allow chain extension, adoption of the β-pleated sheet conformation and aggregation of the β-chains. The citric acid back-titration experiments in TFE suggest that, in both the intra- and the interchain Al^{3+}-complexes, the ensemble of ligand groups of the neurofilament peptides and phosphopeptides have higher affinity toward Al^{3+} than the OH and COOH groups of citric acid. The enhanced affinity toward Al^{3+} can be explained by the greater flexibility of the OH, COO^- and/or PO_3H^- ligand groups of the peptides or by the effect of other complex-stabilizing interactions (e.g., the salt bridge fixing the semicyclic structure of the intrachain complex (see Fig. 6A). The importance of electrostatic interactions is emphasized by

the observation that NF-M17 shows characteristic β-sheet shifts of the CD spectra in TFE upon addition of increasing amounts of Ca^{2+}, while NF-M17-NH_2, lacking the C-terminal negatively charged carboxylate, does not [41,42].

Prompted by the results of the CD titrations on Ala-substituted NF-M17 derivatives, analogues were synthesized containing five alanine residues (in positions 1, 2, 6, 14, 15, as well as 1, 2, 11, 14, 15, and 6 or 11) and only one serine or phosphoserine (in position 6 or 11). Ca^{2+} and Al^{3+} titration experiments strongly supported our earlier findings that (1) Al^{3+} has a much higher binding affinity to neurofilament peptides than does Ca^{2+}; and (2) the conformational effect of the two cations is significantly different. Most interestingly, the strongest Ca^{2+}-induced β-sheet shift of the CD spectra was observed for NF-M17($A^1A^2A^{11}A^{14}A^{15}$), with one Ser in position 6. These and other Ca^{2+} titration data measured on alanine derivatives [82] suggest that nonprotonated lysines may also be involved in Ca^{2+} binding, as proton acceptors. Aluminum proved to be less effective than calcium: the strongest and practically irreversible β-sheet shift was seen in the case of NF-M17($A^1A^2A^{11}A^{14}A^{15}$-S^6P). These and other Ca^{2+}-titration data, measured on alanine derivatives [82], suggest that nonprotonated lysines may also be involved in Ca^{2+}-binding.

The roughly five orders of magnitude difference in the stability of the citric acid Al^{3+} and Ca^{2+} complexes in aqueous solution [83] suggests that in a decreased dielectric constant environment (e.g., in the solvent TFE [89] used in our experiments or in certain areas of the neuron), Al^{3+}-binding is practically irreversible. Consequently, Al^{3+} intoxication is expected to have a long-lasting or delayed effect. It is reasonable to suggest that the formation of intrachain complexes protects the proteineous neurofibrillary structures from the β-sheet transition and aggregation, while that of interchain complexes have an opposite effect, namely a β-sheet inducing effect. Another interesting finding is that Ser-phosphorylated neurofilament fragments always form interchain complexes, with a β-sheet conformation in the presence of both Ca^{2+} and Al^{3+} ions.

The formation, possible structure and conformational role of interchain complexes have been reported [42]. A molecular mechanism for Al^{3+}-induced neurofilament bundling has been suggested by Leterrier et al. [21]. This mechanism assumes the formation of an intramolecular and an intermolecular Al^{3+}-complex. It is the latter complex that may be responsible for the conformational changes resulting in a decreased electrophoretic mobility of the NF-M and NF-H subunits [21]. According to this hypothetical model, the intrachain complex is formed at low, while the interchain complex is formed at high NF concentrations. Our studies revealed the role of the OH groups of serine in stabilizing the intramolecular complex, which makes possible a molecular explanation for the existence of two types (intra- and inter-molecular) of Al^{3+} binding modes to NF-M protein fragments.

The finding that the Ser-phosphorylated neurofilament peptides form exclusively intermolecular Al^{3+}-complexes, with a clear-cut β-sheet forming tendency [34,41], strongly emphasizes the importance of phosphorylation in β-sheet formation and aggregation. In vivo aluminum treatment was found to alter neurofilament protein phosphorylation [73,78,89]. It has been reported recently that aluminum can induce nonenzymatic incorporation of the α- and γ-phosphates of ATP, GTP and CTP into

the human tau protein [17]. It was suggested that the complexing of Al^{3+} by the negatively charged phosphate oxygens may be involved in catalyzing nonenzymatic phosphorylation [17]. The participation of the serine OH in binding to Al^{3+} in the intrachain peptide complexes (e.g. Fig. 6(A)) offers an alternative explanation. It is the enhanced nucleophilicity of the complexed oxygen of the serine OH, and the possibility of nucleotide triphosphate binding to the same Al^{3+}, that may play a role in the nonenzymatic phosphorylation reaction. The tau protein [90], in Alzheimer's paired helical filaments, is hyperphosphorylated at multiple sites, e.g., in the KSPV tetramer [91]. Tau has many regions in its sequence [92] which are rich in serine(s) and neighboring acidic residues (glutamates or aspartates). Al^{3+}-induced phosphorylation, with the participation of an intrachain Al^{3+}-complex, may be the crucial step which promotes phosphorylation of tau and opens the route that leads to tangle formation.

There are several indications that the concentration of aluminum is not elevated significantly in Alzheimer's plaques [13,15,93], which suggests that it plays an etiologic role only in tangle formation. However, there is equally strong evidence of the involvement of aluminum in plaque formation [93–95]. Aluminum was found to accelerate proteolytic processing of the amyloid precursor protein by suppression of the inhibitor domain [95a]. Furthermore, it was also reported to destroy the partial helical conformation of βA4(1–40) peptide in a membrane-mimicking environment [96]. The sequence homology between the amyloid precursor protein (APP) and regions of the human neurofilament triplet protein [97] represents another link between the tangle and plaque aggregates in Alzheimer's disease. Our studies support the idea that aluminum, as a possible seed or template, or a catalyst, promotes aggregation which may lead either to tangle or plaque formation (Fig. 6(C)).

Aluminum is an abundant element in the earth, and biological evolution occurred at relatively high aluminum levels. Natural complexing ligands (e.g., nucleic acids, nucleotide triphosphates, hydroxy acids, or regions of proteins and other molecules which are rich in acidic and hydroxy functions) have probably served as buffer systems to protect functional regions of the brain and other tissues from aluminum intoxication. Environmental aluminum is bound in low-solubility compounds and inorganic complexing agents (hydroxy, fluoride, etc.), which have been involved in maintaining the concentration of "biologically available aluminum" below a critical level. However, geological, technological, cultural, dietary and medical factors [13,97,98] may have led to temporary or permanent exposure to high aluminum levels. Al^{3+} concentrations between 0 and 0.6 ppm (dry weight) have been measured in normal human brain. In the brains of Alzheimer's patients, the concentration of Al^{3+} ranges between 0 and 15 ppm in nondegenerated regions but between 6 and 12 ppm in areas containing neurofibrillary lesions [99]. The most significant conclusion of our studies is that aluminum, due to its strong complexing ability, may accumulate in proteinous structures of the nerve cells, and above a critical level it may trigger a variety of molecular events which, through aggregation steps, lead to tangle or plaque formation.

Calcium has a lower affinity for the majority of natural ligands than does aluminum. While a temporary complexing and concomitant conformational effect of

elevated calcium is easily antagonized by the natural ligand molecules of the cytosol, extracellular space, or body fluids, aluminum has a long-lasting, practically irreversible effect on biomolecules that may overcome the "buffer capacity" of the natural ligands. Our data, together with an abundance of evidence in the recent literature, strongly suggest that limited human exposure to unnecessarily high aluminum concentrations might be expected to increase the incidence of Alzheimer's and other aluminum-related neurodegenerative diseases.

5. Alanine-substituted C-terminal domain of NF-M binding sites for metals [82]

A study was undertaken to characterize the cation binding and unphosphorylated NF-M13 and NF-M17 peptides and their analogues in which the glutamates, or one or both of the serine residues, were replaced by alanine (Table 2) [82]. NF-M13, NF-M17, and their phosphorylated derivatives, representing the C-terminal phosphorylation domain of the neurofilament protein midsize subunit, have four possible binding sites for metal ions; the COO^- group of glutamate, the OH group of the serine residue, the PO_3H^- group of phosphoserine (when present), and the COO^- at the terminus of the peptide chain. The CD titration of the phosphorylated neurofilament fragments with Al^{3+} and Ca^{2+} yielded a significant conformational change which resulted in conformations containing high β-pleated sheet contents, which precipitate on standing (intermolecular complex). Al^{3+} binding to the unphosphorylated NF-M13 and NF-M17 did not exhibit this behavior. Several alanine analogues of the parent NF-M17 peptide were synthesized in order to determine the relationship between metal ions and possible binding sites. CD titration of analogues with Ca^{2+} indicated that the critical residues of NF-M17 for Ca^{2+}-induced conformational changes, from random to β-pleated sheet, are the N-terminal serine or both phosphorylated serines. Al^{3+}-induced conformational changes suggest that the critical sites of NF-M17 yielding the β-pleated sheet structure are the four glutamates or phosphorylated serines, especially the C-terminal SerP. Based on the titration data, it is very likely that analogues with a serine in position 11 form a stable intramolecular complex with Al^{3+} which, however, does not result in the adoption of the β-conformation. Back-titration with citric acid fails to reverse the Al^{3+}-induced conformational changes of the phosphorylated peptides. The above results, especially the possible formation of intramolecular and intermolecular Al^{3+} complexes, may have relevance to the molecular mechanism through which the neurotoxin Al^{3+} gives rise to the formation of neurofilament tangles.

5.1. Ca^{2+} and Al^{3+} titration and citric acid back titration of nonphosphorylated NF-M13 and NF-M17

CD titration of unphosphorylated NF-M13 or NF-M17 in TFE, with Ca^{2+} induced a conformational change of random coil to β-sheet. (For preliminary data, see Hollósi et al. [41,42].) The intensity of the negative trough near 205 nm decreased with the increase of the $[Ca^{2+}]/[pep]$ ratio (r_{Ca}). At $r_{Ca}=2$, the 205 nm band almost vanished, the 220 nm trough did not change, and the positive band shifted to

Table 2
Circular dichroism spectra of NF-M17 and Ala analogues in TFE

Peptide abbreviation	Model	Conformational change based on CD spectra[a]	[metal ion]/[peptide] ratio	CD parameters in TFE					
				nπ* band		λ (nm)	ππ* bands		$[\theta]_M$
				λ (nm)	$[\theta]_M$		$[\theta]_M$	λ (nm)	
NF-M17	^{1}EEKG^{5}KSPVP^{10}KSPVE^{15}EKG		no metal ion	220	−3200	203	−5000	185	5000
			[Ca]/[pep] = 2	220	−3200	205[c]	−2000	188	6500
		I→β	[Ca]/[pep] = 4	219	−2800	205[c]	−1300	185[b]	3800
		β→I (rev)	[cit]/[Ca] = 4	220	−3000	203	−5000	185	5000
		I→M	[Al]/[pep] = 16	218	−3200	202	−3400	185	3700
		no change	[cit]/[Al] = 8	218	−3100	202	−3200	185	3100
NF-M17($S^{6}PS^{11}P$)	EEKGKS(·PO_3H_2)PVPKS(·PO_3H_2)PVEEKG		no metal ion	218	−4500	203	−5000	185	3300
		I→M	[Ca]/[pep] = 16	218	−4000	203[c]	−3300	185	3300
		M→R	[cit]/[Ca] = 16	218	−3000	198	−4100	185	2200
		I→β	[Al]/[pep] = 8	218	−5300	203[b]	−4000	185	5000
		no change	[cit]/[Al] = 16	218	−4900	203[b]	−3600	185	5000
NF-M17($A^{6}A^{11}$)	EEKGKAPVPKAPVEEKG		no metal ion	221	−3000	200	−4500	185	1300
		I→R	[Ca]/[pep] = 16	221[c]	−2000	196.5	−5600	185	800
		R→I (rev)	[cit]/[Ca] = 16	221	−3000	200	−4700	185	2000
		I→M(β)	[Al]/[pep] = 16	216	−4200	200[b]	−2700	185	2700
		no change	[cit]/[Al] = 8	218	−3300	200	−2900	185	2500
NF-M17(A^{6})	EEKGKAPVPKSPVEEKG		no metal ion	218	−3000	201.5	−4300	185[b]	2100
		I→R	[Ca]/[pep] = 16	216	−1850	196	−4000	185[b]	2100
		R→I (rev)	[cit]/[Ca] = 16	218	−2800	201	−4300	185[b]	2100
		I→M	[Al]/[pep] = 16	215[c]	−4100	201.5[c]	−4000	185[c]	3100
		no change	[cit]/[Al] = 12	216	−3950	201.5	−3900	185[c]	3100
NF-M17($A^{6}S^{11}P$)	EEKGKAPVPKS(·PO_3H_2)PVEEKG		no metal ion	218	−3000	205	−3400	186	2200
		I→R	[Ca]/[pep] = 16	216[c]	−2800	200	−3400	186	3000
		M(R)→I	[cit]/[Ca] = 16	218	−3000	196	−6100	186[c]	1500
		I→M(β)	[Al]/[pep] = 16	218	−4250	205[c]	−3500	186	4500
		M(β)→M	[cit]/[Al] = 16	218	−3300	205[c]	−2400	186	6000
NF-M17(A^{11})	EEKGKSPVPKAPVEEKG		no metal ion	218	−3800	200	−6300	186	1900
		I→M	[Ca]/[pep] = 16	218	−3400	197	−4800	186[b]	3500
		M→I (rev)	[cit]/[Ca] = 16	218	−3600	199.5	−6500	186	3000
		I→M(β)	[Al]/[pep] = 16	218	−4600	200	−5300	186	2000
		M(β)→M	[cit]/[Al] = 4	218	−4500	201	−4800	186	3500
NF-M17($S^{6}PA^{11}$)	EEKGKS(·PO_3H_2)PVPKAPVEEKG		no metal ion	218	−3300	200	−4900	186	1800
		I→β	[Ca]/[pep] = 16	218	−3200	200[c]	−2900	187	3000
		β→I (rev)	[cit]/[Ca] = 16	218	−3100	200	−4900	186	2400
		I→M(β)	[Al]/[pep] = 16	218	−4100	200[c]	−3000	186	2000
		M(β)→M	[cit]/[Al] = 16	218	−3500	200[c]	−2000	186	4000

NF-M17($A^1A^2A^{14}A^{15}$)	AAKGKSPVPKSPVAAKG			no metal ion	220[c]	−3200	201	−6000	185[b]	1500
				[Ca]/[pep] = 2	220	−3200	202[b]	0	192	3800
			I−β	[Ca]/[pep] = 3	220	−2400	201[b]	0	192	2000
			β→I (rev)	[cit]/[Ca] = 2	220[c]	−3000	200	−5700	185[b]	2000
			I→M(R)	[Al]/[pep] = 8	220[c]	−2200	197	−4900	185[b]	0
			M(R)→M	[cit]/[Al] = 16	220[c]	−3000	202	−4600	185[b]	2200
NF-M17($A^1A^2A^{14}A^{15}S^6P$)	AAKGKS(·PO_3H_2)PVPKSPVAAKG			no metal ion	220	−2500	200	−4700	185[b]	3500
			I→M	[Ca]/[pep] = 16	220	−2300	200	−5200	185[b]	4400
			no change	[Al]/[pep] = 8	220	−2200	199	−4500	185[b]	3500
			no change	[cit]/[Al] = 8	220	−2500	201	−4500	185[b]	3500
NF-M17($A^1A^2A^{14}A^{15}$)$S^{11}P$)	AAKGKSPVPKS(·PO_3H_2)PVAAKG			no metal ion	219	−3000	199	−4300	185[b]	800
			I→M	[Ca]/[pep] = 16	219	−1200	199	−2100	185[b]	800
			M(R)	[cit]/[Ca] = 16	219	−2600	199	−4700	185[b]	3500
			I→M(I)	[Al]/[pep] = 14	219	−3200	201	−3800	185[b]	1100
			no change	[cit]/[Al] = 8	219	−3100	202	−3300	185[b]	2600
NF-M17($A^1A^2A^{14}A^{15}S^6PS^{11}P$)	AAKGKS(·PO_3H_2)PVPKSPVAAKG			no metal ion	219	−3400	201	−4900	185[b]	1000
			I→M(β)	[Ca]/[pep] = 8	219	−2200	201	−700	188	1000
			M(β)→M(R)	[cit]/[Ca] = 8	219	−2200	201	−3800	188[b]	1000
			I→M	[Al]/[pep] = 8	220	−3400	201	−3500	185[b]	1200
			no change	[cit]/[Al] = 16	219	−3400	201	−3500	185[b]	1200

[a] The same conformational changes were observed at lower [cation]/[pep] and [cit]/[cation] ratios. I, initial conformation; β, β-pleated-sheet dominated conformation; M, mixture of conformers or conformational regions; R, random (aperiodic or unordered) dominated conformation; M(R) and M(β), spectra reflect shifts to random or β-conformation; M(I), small conformational change.

[b] No band.

[c] Shoulder.

~190 nm. The Ca^{2+}-induced conformational change of NF-M13, from random coil to β-sheet, was reversible when back-titrated with citric acid.

In the presence of Al^{3+}, until the $[Al^{3+}]/[pep]$ (r_{Al}) ratio increased to 4, the CD titration of NF-M13 and NF-M17 showed much smaller conformational change than was induced by Ca^{2+}. At $r_{Al}=1$, the CD spectrum was similar to the original spectrum without Al^{3+}. Even at $r_{Al}=4$, the intensity of all three bands did not change significantly. The spectral effect of Al^{3+} was not reversed by citric acid.

The Ca^{2+} complexes of the phosphorylated NF-M13 and NF-M17 peptides were dissociated upon the addition of citric acid; however, in the presence of citric acid, the spectra measured showed characteristic differences relative to the spectra of the parent peptide (without Ca^{2+} and citric acid). For the conformational changes induced by the cations and citric acid, see Table 3.

5.2. Al^{3+} titration and citric acid back-titration of phosphorylated NF-M13 and NF-M17

In agreement with the data reported for the phosphorylated NF-M17 peptides [41], the Al^{3+} titration of the various phosphorylated NF-M13s showed spectral changes which were similar to those induced by Ca^{2+} ions. Based on a comparison of the CD titration data, Al^{3+} is superior to Ca^{2+} in inducing a spectral change reflecting the adoption of the β-sheet conformation.

Al^{3+}-induced conformational changes of the phosphorylated NF-M13 peptides, from random coil to a β-pleated sheet structure, were not reversed when back-titrated with citric acid. The original spectra were not recovered in the case of NF-M13 and NF-M13(Ser^7P) but, upon the addition of citric acid, the spectra showed definite changes. A similar non-reversibility, upon addition of citric acid, was also observed for the phosphorylated NF-M17 peptides (Table 3).

5.3. Ca^{2+} and Al^{3+}-induced conformation transitions of alanine-substituted unphosphorylated fragments

CD monitored Ca^{2+}- and Al^{3+}-binding studies were performed on NF-M17 and its alanine-substituted unphosphorylated analogues NF-M17(A^6A^{11}) and NF-M17($A^1A^2A^{14}A^{15}$). Ca^{2+} and Al^{3+} had strikingly different spectral effects on the serine- and glutamate-substituted peptides. In the case of NF-M17 and NF-M17($A^1A^2A^{14}A^{15}$), addition of Ca^{2+} ions at $r_{Ca}>2$ resulted in significant increase of the β-pleated sheet conformer populations (Table 3). The spectra changed gradually but at $r_{Ca}>4$, the intensity of both the negative and positive bands began to decrease due to precipitation of the complex and the concomitant concentration decrease in the solution. (A similar behavior was observed earlier and reported [41,100].) The β-pleated-sheet content was calculated to be more than 40% at ratio 2 (Table III). The increase of β-content was accompanied by a comparable decrease of the random conformation.

Upon addition of Al^{3+} ions, NF-M13, NF-M17, and NF-M17($A^1A^2A^{14}A^{15}$) failed to yield β-pleated sheet spectra, even at $\geq r_{Al}=8$. The spectrum of the $A^1A^2A^{14}A^{15}$ analogue reflected increasing amounts of random conformation (~50% at $r_{Al}=8$).

Table 3
Secondary structure of NF-M17 Ala analogues with Ca^{2+} and Al^{3+} and their reversibility with citric acid [68]

Peptide abbreviation	[metal ion]/[peptide] or [citric acid]/[metal ion] ratio	α-helix (%)	β-sheet (%)	random (%)	error/46 points
NF-M17	no metal ion	4	36	60	0.45
	[Ca]/[pep] = 2	6	42	52	0.45
	[cit]/[Ca] = 4	4	45	51	0.35
	[Al]/[pep] = 16	3	40	58	0.27
	[cit]/[Al] = 8	4	39	57	0.28
NF-M17($S^6PS^{11}P$)	no metal ion	5	35	60	0.40
	[Ca]/[pep] = 16	5	38	57	0.38
	[cit]/[Ca] = 16	1	42	58	0.30
	[Al]/[pep] = 16	3	47	50	0.35
NF-M17(A^6A^{11})	no metal ion	1	40	60	0.42
	[Ca]/[pep] = 16	0	38	62	0.61
	[cit]/[Ca] = 16	1	39	60	0.33
	[Al]/[pep] = 16	5	39	56	0.03
	[cit]/[Al] = 8	4	40	57	0.22
NF-M17(A^6)	no metal ion	2	39	59	0.48
	[Ca]/[pep] = 16	0	41	59	0.67
	[cit]/[Ca] = 16	1	39	60	0.48
	[Al]/[pep] = 16	4	37	59	0.03
	[cit]/[Al] = 12	4	37	59	0.05
NF-M17($A^6S^{11}P$)	no metal ion	3	40	57	0.35
	[Ca]/[pep] = 16	2	49	59	0.31
	[cit]/[Ca] = 16	0	39	61	0.82
	[Al]/[pep] = 16	5	38	57	0.08
	[cit]/[Al] = 16	5	42	53	0.39
NF-M17(A^{11})	no metal ion	1	36	60	0.14
	[Ca]/[pep] = 16	0	40	60	0.09
	[cit]/[Ca] = 16	1	35	64	0.14
	[Al]/[pep] = 16	2	37	61	0.04
	[cit]/[Al] = 16	3	37	60	0.07

NF-M17(S^6PA^{11})	no metal ion	2	37	61	0.22
	[Ca]/[pep] = 16	3	40	57	0.23
	[cit]/[Ca] = 16	1	37	62	0.35
	[Al]/[pep] = 16	4	39	57	0.07
	[cit]/[Al] = 16	6	41	54	0.35
NF-M17($A^1A^2A^{14}A^{15}S^6P$)	no metal ion	0	40	60	0.63
	[Ca]/[pep] = 16	0	38	62	0.56
	[Al]/[pep] = 8	1	38	61	0.32
	[cit]/[Al] = 8	3	37	60	0.29
NF-M17($A^1A^2A^{14}A^{15}S^{11}P$)	no metal ion	0	40	60	0.25
	[Ca]/[pep] = 16	0	45	55	1.13
	[cit]/[Ca] = 16	0	40	60	0.28
	[Al]/[pep] = 14	2	39	59	0.23
	[cit]/[Al] = 8	3	40	57	0.39
NF-M17($A^1A^2A^{14}A^{15}S^6PS^{11}P$)	no metal ion	2	37	61	0.19
	[Ca]/[pep] = 8	2	46	52	0.63
	[cit]/[Ca] = 8	1	40	59	0.52
	[Al]/[pep] = 8	3	40	58	0.20
	[cit]/[Al] = 16	3	39	58	0.24
NF-M17($A^1A^2A^6A^{14}A^{15}$)	no metal ion	1	36	63	0.18
	[Ca]/[pep] = 4	3	45	52	1.75
	[Ca]/[pep] = 16	0	59	41	1.60
	[cit]/[Ca] = 4	1	35	64	0.25
	[Al]/[pep] = 16	1	41	58	0.21
	[cit]/[Al] = 8	3	37	60	0.25

According to the CD curve deconvolution data, listed in Table 3, all peptides and phosphopeptides used in this study feature a β-pleated sheet/unordered type conformation, a finding which is supported by FT-IR measurements on phosphorylated NF-M17 fragments [100].

The alanine-substituted serine peptide NF-M17(A^6A^{11}) behaved differently upon addition of Ca^{2+} and Al^{3+} ions. Between $r=8$ and 16, the spectral changes became smaller. The calculated random coil content at $r_{Ca}=16$ was 62%, which is only slightly larger than that calculated from the original curve. In contrast, Al^{3+}-binding by the (A^6A^{11}) analogue leads to gradual shifts toward β-pleated sheet spectra, a trend exhibited upon addition of Ca^{2+} ions to NF-M13, NF-M17, and NF-M17($A^1A^2A^{14}A^{15}$), but not with NF-M17(A^6A^{11}). Apparently, Ca^{2+}-binding to the carboxylate ligands of glutamate does not play a significant conformational role. By contrast, Al^{3+}-binding appears to cause a shift toward the β-pleated sheet only in the case of NF-M17(A^6A^{11}) containing carboxylate but no hydroxy side-chain groups.

The ligand space of Ca^{2+} and Al^{3+} is different [88]. It is surprising, nevertheless, that the Ca^{2+}- and Al^{3+}-induced conformational transitions have quite different mechanisms. At least in the case of NF-M17(A^6A^{11}), the Al^{3+}-induced β-pleated sheet formation appears to be directly connected with Al^{3+}-complexing, probably through Al^{3+} cross-bridges between carboxylates from different molecules. In contrast with this, Ca^{2+} ions do not form β-promoting cross-bridges with the same carboxylate groups. To characterize the importance of the C- and N-terminal serine residues in cation binding and β-pleated sheet formation, titration experiments were also performed on the alanine analogues NF-M17(A^6) and NF-M17(A^{11}) (with four glutamates), as well as NF-M17($A^1A^2A^6A^{14}A^{15}$) and NF-M17($A^1A^2A^{11}A^{14}A^{15}$) (with Ala replacing Ser^6 or Ser^{11} and Glu at each position). Ca^{2+}-binding by NF-M17(A^6) or NF-M17(A^{11}) resulted in no clear-cut conformational changes. The spectra, measured at high r_{Ca} values, reflected only small shifts. Within this group of models, binding of Ca^{2+} induced the most significant conformational change toward the β-pleated sheet structure in NF-M17($A^1A^2A^{11}A^{14}A^{15}$) (with Ser at 6). This suggests that the N-terminal serine is more important than the C-terminal serine for Ca^{2+}-induced β-pleated sheet formation. Al^{3+}-binding at high r_{Al} values yielded subtle spectral transitions (Tables 2 and 3).

5.4. Cation-induced conformational transitions of phosphorylated alanine-substituted NF-M17 fragments

The alanine-substituted monophosphate NF-M17($A^6S^{11}P$) did not show a definite conformational effect in the presence of Ca^{2+} (Tables 2 and 3). This disagrees with earlier results on monophosphorylated NF-M17 derivatives showing a position-dependent (6 or 11) but significant β-pleated sheet formation upon Ca^{2+}-binding at $r_{Ca}>5$. In the isomeric (S^6PA^{11}) phosphopeptide, Ca^{2+}-binding gave rise to some (37 to 40%) increase of the β-pleated sheet content.

Al^{3+} was found to be an efficient β-sheet promoter in the case of diphosphate models. A marked conformational change (I→β) was observed for NF-M17($S^6PS^{11}P$)

at $r_{Al}=8$ (Tables 2 and 3). The ($A^6S^{11}P$) and (S^6PA^{11}) monophosphates showed weak and position-dependent Al^{3+}-sensitivity, with a stronger β-pleated sheet promoting effect of the latter peptide. The mono- and diphosphorylated NF-M17($A^1A^2A^{14}A^{15}$) peptides also showed low and position-dependent cation sensitivity (Tables 2 and 3).

Citric acid back-titration experiments on alanine-substituted peptides (Table 2) are consistent with our earlier findings, which showed that citric acid is an excellent chelator that can overcome the affinity of unphosphorylated and phosphorylated peptides to Ca^{2+}. In TFE, the Ca^{2+}-induced conformational changes were reversible.

In aqueous solution, the stability of the [Ca^{2+}·cit] complex is relatively low [$\log K_s=3.5$ in water at 0.15 M ionic strength [85, 91], 3.15 at pH = 9.15 in 0.1 M aqueous $Na_2B_4O_7$ buffer or 2.85 at pH = 7.3 in the same buffer (adjusted with HCl). NF-M13(S^2P) has a $\log K_s<1$ with Ca^{2+} in aqueous $Na_2B_4O_7$ buffer at pH = 7.3. This suggests that hydrated Ca^{2+} ions have only weak binding affinity to the peptide ligand groups.

Contrary to this, the Al^{3+}-induced conformational changes were not affected by the addition of citric acid. In TFE, complexing of Al^{3+} ions gave rise to transitions toward the β-pleated sheet conformation in the case of NF-M17(A^6A^{11}) and NF-M17($S^6PS^{11}P$) (Table 2). NF-M17(A^{11}) still showed some β-pleated sheet formation, but the other models listed in Table 3 resulted in no definite spectral changes towards β-sheets ($I\rightarrow\beta$). Most importantly, the effect of Al^{3+} ions could not be reversed by citric acid, regardless of the type of conformation induced. The consistent failure of adopting the β-pleated sheet conformation by peptides featuring a C-terminal serine residue (in position 7 in the 13-mer and 11 in the 17-mer, respectively) strongly emphasizes the role of the OH function of serine(s) in a type of Al^{3+}-complexing which does not lead to the β-pleated sheet conformation.

Citrate binding of Al^{3+} is discussed in several reports. For a critical evaluation of the stoichiometries and stability constants of the Al^{3+}-complexes, see Refs. [81,88]. At pH < 8 values, the predominant complex species is [Al·citH_{-1}]$^-$, in which the citrate serves as a tridentate ligand with two carboxylates and a deprotonated hydroxy group. The ligand function of a deprotonated hydroxy group is strongly supported by X-ray crystallographic data on Al^{3+} complexes of hydroxy acids [84–87]. The other species which, at high citric acid excesses, gives a contribution to the complex equilibrium between pH 5–7.5 is [Al·cit$_2$]$^{3-}$. The citric acid back-titration data on the NF peptides and phosphopeptides, featuring a C-terminal serine, suggest the adoption of a C-terminal type [Al·pepH_{-1}]$^{-1}$ complex. In this intramolecular (intrachain) complex the backbone is folded and the ligand groups are attached to a semicyclic peptide chain [84]. It is the stable, folded structure of the complex that prevents the extension of the chain and the formation of interchain complexes.

The use of TFE and other halogenated solvents, either as membrane mimetics or as an environment with helix-promoting ability, may be due to the duality of their low dielectric constant and high dipole moment [101] (chlorethanol, $\varepsilon=25.8$, D = 1.90; TFE, $\varepsilon=26.6$) [89]. Ethanol with $\varepsilon=25$ and D = 1.71 has no helix-inducing effect. It is likely that the higher dipole moment of halogenated alcohols is responsible

for the unfolding of the peptide chain and refolding into an α-helical conformation. The CD spectra of phosphorylated and nonphosphorylated NF-M fragments have been found to have some helical character in TFE [42,58]. The peptides, themselves, have no intrinsic potential to form β-pleated sheets. Thus, the α to β conformational transition is clearly the consequence of multivalent metal ion binding. The main role of TFE may be that it cannot solvate metal ions as effectively as water does, which probably increases the stability of the metal ion bridges. However, the relatively low dielectric constant may also stabilize the new system of H-bonds between the extended peptide chains. In TFE, Al^{3+} is expected to form more stable complexes with citric acid than in aqueous buffers. It follows from the failure of the citric acid back-titration experiments that the global $\log K_s$ values of $[Al{\cdot}pepH_{-1}]^{-1}$ type complexes in TFE are probably higher than 8.1, which is the value of the $[Al{\cdot}citH_{-1}]^{-1}$ complex in water.

Al^{3+} titration data on NF-M17(A^6A^{11}) and NF-M17(A^{11}) give strong support to the ligand function of the OH group in position 11. In models lacking this OH group, the intrachain complex cannot be formed. Instead, Al^{3+} ions cause chain extension and most likely the formation of Al^{3+}-bridged β-pleated sheet conformation. It is likely that the N-terminal EE...S^6 triad also has the ability for intrachain Al^{3+}-complexing, but the stability of this complex is probably lower and cannot prevent β-pleated sheet formation at higher r_{Al} values.

The mono- and diphosphates of NF-M17-amide [42] and NF-M13 were found to show β-pleated sheet forming tendencies upon binding of Ca^{2+} or Al^{3+} ions. Generally, a definite increase of the amount of β-pleated sheet was observed only at r_{Ca} and $r_{Al} > 5$. NF-M17(S^6P) (termed S^2P) [42] also showed a β-pleated sheet capability. However, in concert with the data herein, the (S^6P) phosphopeptide was a weaker β-pleated sheet former than its ($S^{11}P$) isomer, lacking the C-terminal serine needed for the intrachain $[Al{\cdot}pepH_{-1}]$ type complex.

These findings, together with the Al^{3+}-titration data on phosphopeptides of NF-M17($A^6S^{11}P$), ($A^{11}S^6P$), and ($S^{6,\ 11}P$) (Table 2), support the existence of a second interchain $[Al^n{\cdot}pep_2]$ type of complex (n is the number of the possible binding sites along the peptide chain) [80], which is formed with the participation of two or more peptide chains. This complex allows chain extension and further association of the β-pleated sheet strands to form a complete β-pleated sheet conformation. In the $[Al^n{\cdot}pep_2]$ type complex, which may correspond to the $[Al{\cdot}cit_2]^{3-}$ complex, the β-chains are cross-linked with Al^{3+}-bridges. Based on the coordination chemistry of aluminum [81] and X-ray crystallographic data on a trinuclear Al^{3+}-citrate complex featuring Al–O–Al bridges with the involvement of the deprotonated hydroxy group of citrate [87], in the $[Al^n{\cdot}pep_2]$ type complex Al^{3+} ions should have acidic ($-PO_3H^-$ and/or COO^-) ligands, but the formation of –O– bridges is also likely. The COO^- side-chain groups of contiguous glutamates (EE) are located above and below the average plane of a β-pleated sheet; therefore, the formation of an Al^{3+}-bridge requires two anionic groups, one from each chain and one Al^{3+} per bridge. Thus, β-pleated sheet formation may need up to five Al^{3+} ions per peptide in NF-M17, having five anionic groups, and seven in NF-M17($S^6PS^{11}P$). This explains the observation that a >5-times excess of Al^{3+} is necessary to reach an r_{Al}

value above which no more β-pleated shift of the CD spectrum is observed. The complex equilibrium is described by the following equation:

$$2[\mathrm{Al{\cdot}pepH_{-1}}]+(n-2)\mathrm{Al^{3+}} \rightleftarrows [\mathrm{Al^{n}{\cdot}pep_2}]$$

where n is the number of Al^{3+} binding sites per peptide (the net charges are not shown). Aggregation of further β-chains results in type $[Al^{m\cdot n}{\cdot}pep_m]$ polycomplexes which stabilize β-sheets cross-linked by Al^{3+}-bridges above and below the plane of the sheet. The CD titration data clearly show that in the case of peptides with one (C-terminal) or two free serine residues, the type $[Al{\cdot}pepH_{-1}]$ intramolecular complex is preferred to the intermolecular ones formed between two anionic groups attached to different peptide chains.

The speculative models of intra- and intermolecular Al^{3+} complexes are in agreement with the CD-monitored Al^{3+}-titration data (Table 2). The citric acid back-titrations indicate that in TFE both the intrachain and the interchain Al^{3+} complexes are stable enough to resist citric acid complexing.

One-dimensional ^{1}H-NMR titrations of the NF-M17 peptide, its unphosphorylated and phosphorylated forms, with Al^{3+} show broadening of the resonances and their coalescence towards a central frequency. Additionally, only 1–2 equivalents of Al^{3+} have been added before precipitation of the peptide–metal complex begins to occur. These results are not promising for extension to two-dimensional methods and full structural characterization of the ion bound form. Comparative FT-IR spectroscopic studies of NF-M17 and NF-M17(A^6A^{11}) give support to the hypothesis of formation of inter- and intramolecular Al^{3+} complexes [82].

To propose a rational explanation for Ca^{2+} complexing and Ca^{2+}-induced conformational transitions is indeed challenging. Ca^{2+}-titration data on NF-M17(A^6A^{11}) showed that a definite β-pleated sheet formation occurs only if the molecule contains both serine residues (Table 2). Ca^{2+} has a more flexible ligand space [81,88] than does Al^{3+}. Moreover, in Ca^{2+}-complexes an OH group does not play as important a role as it does in Al^{3+}-complexes. The finding that in unphosphorylated NF-M13 [42,86] and NF-M17, the spectral transition occurs at $<r_{Ca}<2$ may indicate that the major complex species is of the type $[Ca^{n}{\cdot}pep_2]$ ($n=1$ or 2). The decrease of band intensities seen at $r_{ca}>2$ is due to partial precipitation of the Ca^{2+} complex [42,86]. This dimer may serve as a template for type $[Ca^{m\cdot n}{\cdot}pep_m]$ β-pleated sheet polycomplexes, similar to the case of Al^{3+}-complexes. The low r_{Ca} indicates that electrostatic forces also take part in assembling β-strands to form a β-pleated sheet structure.

Secondary structural prediction showed that the KSPVPKSP domain has practically no tendency to form a continuous β-pleated sheet conformation [29]. This explains why the calculated amount of β-pleated sheet conformation is usually below 50% (Table 3). Fourier-transform infrared (FT-IR) spectroscopic studies on the Ca^{2+} complexes of phosphorylated NF-M17 fragments also showed the presence of significant amounts of the unordered and other conformations in addition to the β-pleated sheet [100]. It is likely that the formation of Ca^{2+} cross-linked β-pleated sheet segments is the cooperative result of favorable electrostatic, complexing, and structural effects. In contrast with Al^{3+}, Ca^{2+} does not have a tendency to form a folded

type [Ca·pep] complex. If the type [Ca^{n}·pep_2] complex cannot be formed, the CD spectrum reflects a shift toward the unordered conformation (increased intensity and blue-shift of the first $\pi\pi^*$ band). In the case of phosphorylated peptides, the spectral shift reflecting the β-pleated sheet conformation occurs at higher r_{Ca} values, which may be taken as a sign of Ca^{2+} cross-linking between more than one pair of anionic COO^- and/or $-PO_3H^-$ groups. Finally, the surprising β-pleated sheet formation by NF-M17($A^1A^2A^{14}A^{15}$), containing no COO^- groups, at $r_{Ca}>2$ may suggest that the major effect of the Ca^{2+} bridges in the glutamate models is due to the screening of the repulsion between the negatively charged groups.

The data discussed herein are believed to also have relevance to the dispute concerning the role of aluminum in the etiology of Alzheimer's disease and other neurodegenerative diseases that are marked by accumulation of β-pleated sheet aggregates. The comparable, or even higher, Al^{3+}-binding affinity in TFE of NF-M fragments, relative to that of citric acid, implies that the C-terminal acidic regions of the NF proteins may bind Al^{3+} with high $\log K_s$ values, even in the natural environment of neurons. However, if the Al^{3+}-complex is of type [Al·pepH_{-1}], then the folded structure does not allow the adoption of the β-pleated sheet conformation.

The C-terminal tail of NF-M proteins has more flexibility than the triple helical N-terminal head domain. It can probably easily tolerate the conformational effect which is caused by intrachain complexing. The major problem is that the intrachain complex is very stable, and the bound Al^{3+} may have a long-lasting effect.

Further accumulation of Al^{3+}, phosphorylation, aberrant degradation, and other factors which also play an essential role in the etiology of AD may, however, lead to the [Al·pepH_{-1}]→[Al^{n}·pep_2]→[Al^{mn}·pep_m] shifts of the complex equilibria and trigger the β-aggregation process. In the [Al^{n}·pep_2] complex, the neighboring chains already have at least a partial parallel or anti-parallel β-orientation. Thus, even a short [Al^{n}·pep_2] double-stranded β-pleated sheet segment may serve as a seed in β-aggregation in a process that resembles that of crystallization. The β-aggregates may also be formed from different proteins (or their proteolytic fragments). The Al^{3+} bridges may also be effective in binding acidic components (e.g. acidic proteoglycans) [43,102], as well as causing different β-filaments to associate. Ca^{2+} ions, due to their lower affinity toward fragments having the same COO^-, $-PO_3H^-$ and OH ligand groups, are less effective. Ca^{2+} is involved in the delicate ion equilibria in the cytosol and a complexing of Ca^{2+}, which induces β-aggregation, requires long-lasting pathologic or age-related exposure to high Ca^{2+} levels. Al^{3+} is a more effective aggregating agent due to the higher stability of its intra- and intermolecular complexes. The strong and/or long-lasting complexing of Al^{3+} places emphasis on the importance of dietary factors (aluminum intake by drinking water, other liquids, foods and drugs) in consideration of the prevention or retardation of Alzheimer's disease and other aluminum-related neurodegenerative diseases.

6. Solubilization of model Alzheimer tangles: reversing the β-sheet conformation induced by aluminum with silicates [103]

Neurofibrillary tangles are one of two lesions found in the brain of Alzheimer's victims. Using synthetic peptide fragments of Human Neurofilament NF-M17 (phos-

phorylated and unphosphorylated), CD studies were performed to examine the effect of sodium orthosilicate on the conformational state produced by Al^{3+} on fragments of neuronal proteins. Previous studies [42] had shown a conformational transition from α-helix and random to β-pleated sheet, upon addition of Al^{3+} to both the phosphorylated and unphosphorylated peptides. If sufficient quantities of Al^{3+} are added, the peptide precipitates from solution. The ability to reverse or slow the progression of aggregation was examined. Al^{3+} binding was reversed with 1–2 equivalents of sodium orthosilicate (with respect to Al^{3+}), altering the conformation from β-sheet to random coil and resulting in a CD spectrum similar to that of the initial peptide. The tight binding of the SiO_4^{4-} with the Al^{3+} provides the mechanism for this transition. These results provide additional information towards the understanding of the role of aluminum in the Alzheimer diseased brain and suggests the investigation of the possible use of silicates as a therapeutic agent.

Previous studies have illustrated a conformational transition from a structure containing small amounts of α-helix and mostly random structure to one that contains β-pleated sheet upon addition of Al^{3+} [42]. Continued addition of metal ion results in precipitation of the peptide. The titrations were performed in TFE to simulate the lower dielectric constant of the interior of the neuron. The identical results were observed by CD in the studies herein. However, addition of SiO_4^{4-} results in a CD spectrum similar to the initial curve, a reversible conformational change from β-pleated sheet to random coil. The reversibility of the NF-M17/Al^{3+} titration is shown in Fig. 7. The NF-M17 peptide was titrated with 16 molar equivalents of Al^{3+}, beginning at 2 equivalents. The initial CD curve showed a peak at 190 nm and a trough at 204 nm with a shoulder at 220 nm (Fig. 7, curve a). Each addition of Al^{3+} resulted in a reduction of the magnitude of the deep trough at 204 nm and an increase of the magnitude of the shoulder at 220 nm, a CD curve characteristic of a β-pleated sheet (Fig. 7, curve b). With each addition of SiO_4^{4-}, the CD curve gradually returned to its original shape, although no significant change was noted with the first few titration points. It was not until the titration approached equal molar quantities of SiO_4^{4-} and Al^{3+} that significant changes were noted, and a CD spectrum similar in shape to the initial one was observed (Fig. 7, curve c). Twelve hours later the same CD spectrum was obtained. As a control experiment, the NF-M17 peptide was titrated with SiO_4^{4-} ion, alone, to see if this had any effect on the native CD spectrum. Minor changes were observed: a slight rise from the baseline and an increase in the peak intensity at 195 nm. These results may imply an increase in random coil content although the overall shape of the CD curve is very similar to that of NF-M17 alone. NF-M17 dissolved in aqueous media yields a CD curve of a random coil.

Titrations were repeated with the NF-M17 phosphorylated derivatives, NF-M17 S^6P, NF-M17 $S^{11}P$, and NF-M17 S^6P $S^{11}P$. The results of the reversibility titration for NF-M17 S^6P are illustrated in Fig. 8. The CD curve (Fig. 8, curve b) indicated that NF-M17 S^6P was converted to a pleated β-sheet with 4 molar equivalents of Al^{3+}. At equal concentrations of SiO_4^{4-} and Al^{3+} the peptide CD spectrum was beginning to resemble the original CD spectrum. Twice as much SiO_4^{4-} as Al^{3+} resulted in a CD spectrum which had a shallower shoulder at 220 nm and a deeper

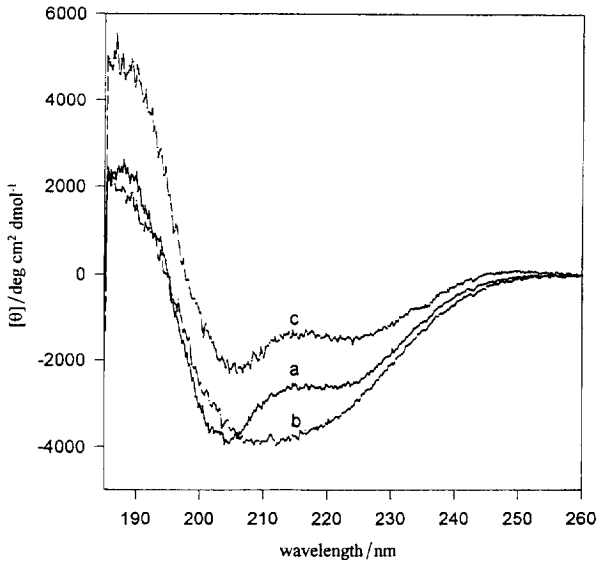

Fig. 7. Reversibility of NF-M17/Al^{3+} titration with SiO^{4-}. Curves: a, NF-M17 at 0.35 mg ml^{-1} dissolved in TFE with no Al^{3+} or SiO^{4-} added; b, same conditions as for curve a but also contains 16 molar equivalents of Al^{3+} and 16 molar equivalents of SiO^{4}. For the CD titrations the peptides were dissolved in TFE at a concentration between 0.4 and 0.18 mg ml^{-1}. The Al^{3+} solutions (aluminum nonahydrate; 33 or 36 mM) were prepared in TFE, and Na_4SiO_4 was dissolved in water (136 mM). Al^{3+} solution was incrementally added until 8 or 16 molar equivalents of metal ion (1 molar equivalent = 5–10 μM) were added to the peptide. Once the maximum conformational change was reached, SiO^{4-} was titrated into the cuvette. Additions were made as increments of peptide molar equivalents (1 molar equivalent = 2–4 μM) and did not exceed 32 molar equivalents [103].

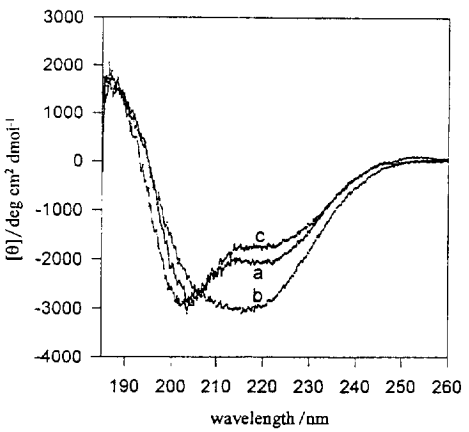

Fig. 8. Reversibility of NF-M17[S^6P]/Al^{3+} titration with SiO^{4-}. Curves: a, NF-M17[S^6P] at 0.4 mg ml^{-1} dissolved in TFE with no Al^{3+} or SiO^{4-} added; b, same as for curve a but also contains 4 molar equivalents of Al^{3+}; c, same as for curve a but also contains 4 molar equivalents of Al^{3+} and 8 molar equivalents of SiO^{4-}. See Fig. 7 for methodology [103].

trough at 204 nm. Titration of the NF-M17 $S^{11}P$ peptide is shown in Fig. 9. After 16 molar equivalents of Al^{3+}, the metal ion titration was complete (Fig. 9, curve b). Reversibility of the Al^{3+} effects required only equal molar quantities of SiO_4^{4-} ion (Fig. 9, curve c); these solution conditions resulted in a CD spectrum with more random character than the original CD spectrum. The NF-M17 S^6P $S^{11}P$ peptide was titrated with 8 molar equivalents of Al^{3+} and required twice as much SiO_4^{4-} ion to obtain a CD spectrum which resembled the peptide alone. These data are presented in Fig. 10. However, previous studies have shown that this peptide appears to bind the Al^{3+} ion more readily [42]. All of these titrations with SiO_4^{4-} gave a random coil-like CD spectrum, the conformation having been converted from the β-pleated sheet.

Evidence has been presented for the reversible binding of aluminum to model peptides from the neurofilament protein, i.e., Al^{3+} can be removed from these peptides using SiO_4^{4-}. Previously, in vitro studies have illustrated that Al^{3+} binds to, and causes the aggregation of, microtubule associated proteins [16], tau protein [17,104], and the peptides derived from the C-terminus of the midsize subunit of neurofilament proteins [42]. Other results have showed that aluminum induces tangle formation in cultured neurons [105,106]. These experiments and data illustrating the presence of aluminum in neurofibrillary tangles [6] lend support to the assumption that aluminum is a risk factor in AD. Thus, the ability to reverse the effects of Al^{3+} binding is an advance in the understanding of the mechanism that brings about tangle formation, and its possible reversal.

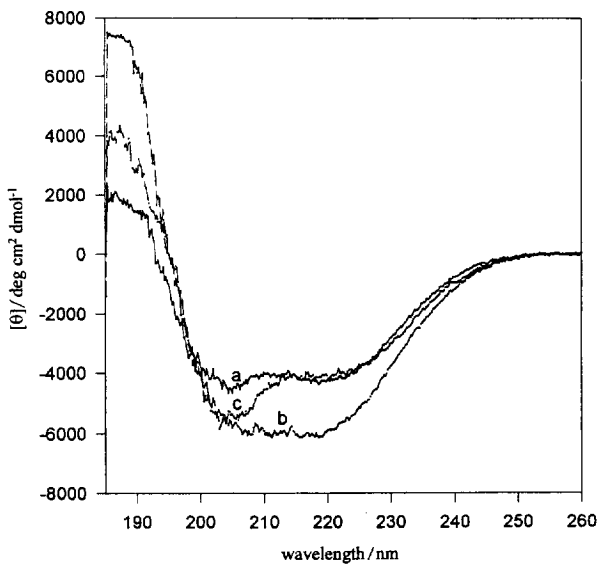

Fig. 9. Reversibility of NF-M17[$S^{11}P$]/Al^{3+} titration with SiO^{4-}. Curves: a, NF-M17[$S^{11}P$] at 0.285 mg ml^{-1} dissolved in TFE with no Al^{3+} or SiO^{4-} added; b, same as for curve a but also contains 16 molar equivalents of Al^{3+}; c, same as for curve a but also contains 16 molar equivalents of Al^{3+} and 8 molar equivalents of SiO^{4-}. See Fig. 7 for methodology [103].

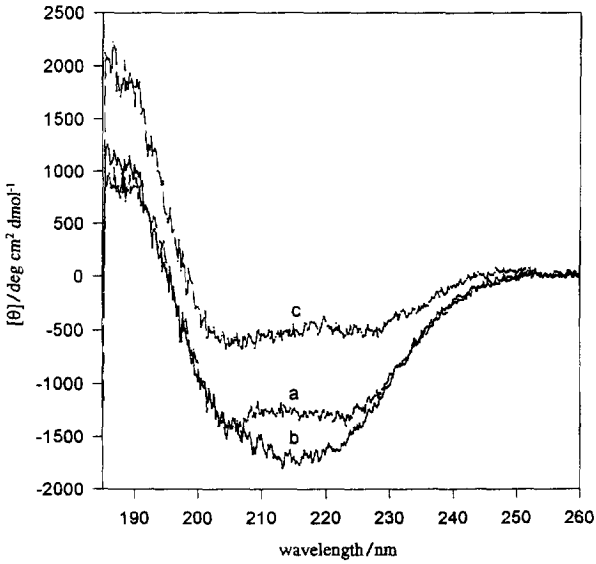

Fig. 10. Reversibility of NF-M17[S^6P, $S^{11}P$]/Al^{3+} titration with SiO^{4-}. Curves: a, NF-M17[S^6P, $S^{11}P$] at 0.365 mg ml^{-1} dissolved in TFE with no Al^{3+} or SiO^{4-}; b, same as for curve a but also contains 8 molar equivalents of Al^{3+}; c, same as for curve a but also contains 8 molar equivalents of Al^{3+} and 16 molar equivalents SiO^{4-}. See Fig. 7 for methodology [113].

The microtubule associated proteins and tau protein have several phosphorylation sites; serine or threonine residues are modified with phosphate moieties, modulating function [17,107]. The presence of negatively charged phosphate groups provides an ideal binding site for Al^{3+}. It has also been shown that γ-COO^- groups of glutamic acid and the –OH of serine can act as ligand sites for Al^{3+} [86]. The polycationic Al^{3+} species draws several possible ligands together, thus aggregating the protein or peptide by formation of β-pleated sheets; this mechanism was put forth from model peptide studies [80].

Silicon, in the form of $Si(OH)_4$, binds tightly to Al^{3+} to form aluminosilicates, particularly at alkaline pH [108]. The beneficial effects of this relationship have been presented by Carlisle and Curran [26], who showed that a silicon supplement to the daily diet slowed or prevented aluminum build up in the aging rat brain. Further, Birchall and Chappell [109] illustrated a reduced aluminum toxicity to Atlantic salmon fry with silicic acid present in the water. The high binding constant of SiO_4^{4-} with Al^{3+} is able to displace the metal ion from the peptides used in these model studies. Birchall and Chappell [110] propose an Si:Al ratio of 0.5 for the formation of an hydroxyaluminosilicate species near physiological conditions. In the studies herein, a Si:Al ratio between 1 and 2 was required for the return of a conformation similar to that of the original peptide. The difference in the ratio is most probably due to changes in solution conditions.

It is hypothesized that silicates may serve as a possible preventative treatment for individuals showing early symptoms of AD or as a method of retarding the advance

of the disease for those individuals already diagnosed with AD. Thus, a rationalization is presented for a similar suggestion by Edwardson et al. [111].

The use of a therapeutic agent to be effective in Alzheimer's disease raises the question of crossing the blood–brain barrier. However, aluminum silicates have been found [7] in Alzheimer's lesions in the brain. Thus, it is evident that both species do cross the blood–brain barrier. It has been shown that dietary silicon supplementation in rats appeared to protect against aluminum accumulation in aging brain [26]. Silicates could be effective in reducing the aluminum concentration in circulating blood, and thus aluminum would be less available to cross the blood–brain barrier. Silicates have been demonstrated to be biocompatible [112].

7. Solubilization of β-amyloid-(1–42)-peptide: reversing the β-sheet conformation induced by aluminum with silicates [113]

Plaques are one of the two lesions found in the brain of Alzheimer's patients. Using a synthetic peptide of A42 (Rat) (βA4), CD studies were performed to examine the effect of sodium orthosilicate on the conformational state produced by Al^{3+}. Fragments of neuronal proteins involved in tangle formation had shown a conformational transition from a β-pleated sheet to a soluble random coil upon addition of Na_4SiO_4. CD measurements showed that the β-pleated sheet conformation of βA4 induced by Al^{3+} was reversed to the random coil soluble form by the addition of Na_4SiO_4. The tight binding of SiO_4^{4-} with Al^{3+} provides the mechanism for this transition. These results provide insight into the role of aluminum in the Alzheimer diseased brain and suggest the investigation of the use of silicates as a therapeutic agent.

In a study of the βA4 peptide (residues 1–42 of the β-amyloid precursor protein), whose prominent role in the progression of AD has been frequently stressed and has been reviewed extensively [113–116], CD studies illustrated the requirements for β-sheet filament formation [117]. Solid state FTIR showed the secondary structure consisted of a β-turn flanked by two strands of antiparallel β-pleated sheet [118]. In aqueous trifluoroethanol solutions, synthetic and naturally occurring β-amyloid peptides, residues 1–42 [β(1–42)] and β(1–39), formed monomeric α-helical structures at high and low pH, as determined by NMR and CD; however, the same study demonstrated that a monomeric β-structure predominated at pH 4–7 [119,120]. The kinetics of aggregation of the synthetic β(1–40) peptide was followed and found to yield two-thirds β-structure but no α-helical structure [121], while a previous study had postulated that Aβ4 aggregates as β-sheets [118]. In addition, it has been reported that aluminum promotes the β-sheet conformation β(1–40) [96] and its aggregation in vitro [122]. Furthermore, the secondary structure of βA4, namely its β-sheet conformation, was necessary to elicit neuro-toxicity in three different assays using rat embryonic neuronal cell cultures [123]. These results and others (see reviews in Refs. [113–115]) support a hypothesis concerning a role of the β-sheet conformation of βA4 and its involvement in the neurodegenerative process of AD. A reversible random coil–β-sheet transition has been demonstrated for the β(25–35)

fragment in aqueous media [89]. However, Fasman et al. [113] have shown that the βA4 β-sheet conformation induced by Al^{3+} (models of plaques in AD) can be reversed or prevented by silicates. A similar experimental approach was previously discussed with model neurofilament peptides (model tangle peptides) [113].

The titration of βA4 (rat) with Al^{3+} and its reversal with SiO_4^{4-} was monitored by far UV-CD to detect any secondary structure changes; these spectra are shown in Fig. 11. At least 45 min passed between the making of the A42 solution or addition of the titrant and the data acquisition, to allow the peptide to reach conformational equilibrium. The initial spectrum, i.e., A42 in trifluoroethanol without Al^{3+} or SiO_4^{4-}, is labeled a in Fig. 11. This curve demonstrates a partial α-helical, partial random coil structure [30]. Upon addition of 2 molar equivalents of Al^{3+}, the $[\theta]_{220}$ increases, indicating the formation of β-sheets (curve b, Fig. 11). On addition of 2 more equivalents of Al^{3+}, the curve (c, Fig. 11) remains identical to the previous one. Similar conformational transitions have been observed previously [96]. Immediately after completing curve c, 2 equivalents of SiO_4^{4-} were titrated into $A42/Al^{3+}$ solution, resulting in curve d of Fig. 11 and causing no detectable change

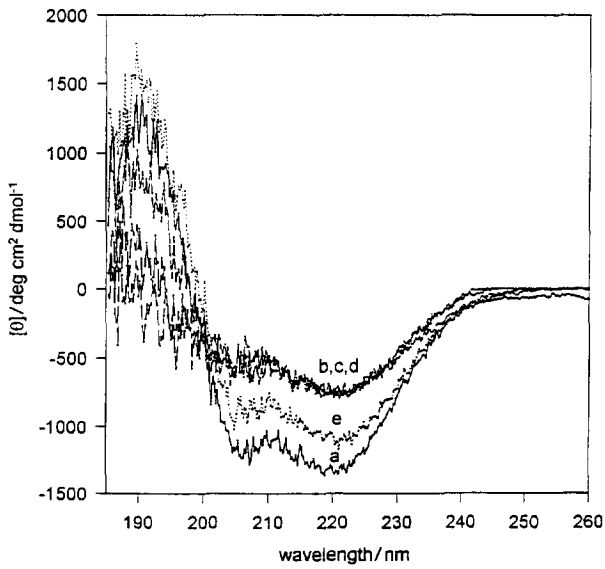

Fig. 11. (a) A42 peptide was synthesized by the solid state synthetic method using Fmoc-N terminal-protecting strategy and a modified M-BHA resin. The peptide was characterized by amino acid analysis, positive ion FAB-MS, and purified by HPLC. The CD titrations were performed in 2,2,2-trifluoroethanal (TFE) (NMR grade). Aluminum perchlorate nonahydrate was purchased from Aldrich; sodium orthosilicate was obtained from Johnson Matthey Catalog Corporation. CD spectra were acquired using a J-Y Mark V Circular Dichrograph. CD titrations of A42 were performed in TFE at concentrations between 0.38 and 0.39 mg ml^{-1}. The Al^{3+} solution (41.6 mM) was prepared in TFE, and Na_4SiO_4 was dissolved in water (138 mM). Initial spectra (a) contained only peptide (conc. = 0.39 mg ml^{-1}). [113]. (b) Same as curve a with 2 equivalents of Al^{3+} and no SiO^{4-} [113]. (c) Same as curve a with 4 equivalents of Al^{3+} and no SiO^{4-} [113]. (d) Same as curve a with 4 equivalents of Al^{3+} and 2 equivalents of SiO^{4-} [113]. (e) Same as curve a with 5 equivalents of Al^{3+} and 4 equivalents of SiO^{4-} [113].

in structure. However, addition of 4 equivalents (total) of SiO_4^{4-} produces curve e, Fig. 11. Thus a reversal of the effect of Al^{3+} was brought about by the addition of SiO_4^{4-}. The β-amyloid (A42) protein, which can be transformed into β-sheets by the addition of Al^{3+}, can be transformed into its initial conformation by the addition of SiO_4^{4-}.

The implications are immediately evident which suggest the possible use of silicates as a therapeutic agent. As both model tangles [113] and precipitated β-pleated sheets of βA4 can be reversed to soluble forms by silicates, the use of silicates as a therapeutic agent for AD is suggested. SiO_4^{4-} has been shown to be biocompatible, and thus no adverse side-effects can be foreseen [124]. The use of a therapeutic agent to be effective in Alzheimer's disease raises the question of crossing the blood–brain barrier. However, aluminum silicates have been found [7] in Alzheimer's lesions in the brain. Thus, it is evident that both species do cross the blood–brain barrier. Silicates could be effective in reducing the aluminum concentration in circulating blood, and thus aluminum would be less available to cross the blood–brain barrier.

Acknowledgement

This research was supplemented by a grant from the National Institutes of Health, Aging Institute. This is publication 1801 from the Graduate Department of Biochemistry, Brandeis University.

References

[1] R.S. Schehr, Bio/Technology, 12 (1994) 140.
[2] G. Perry and M.A. Smith, Clin. Neurosci., 1 (1993) 199.
[3] S.S. Sisodia and D.L. Price, Clin. Neurosci., 1 (1993) 176.
[4] M. Goedert, Trends Neurosci., 16 (1993) 460.
[5] D.P. Perl, Envir. Health Perspect., 63 (1985) 149.
[6] R.L. Bertholf, CRC Crit. Rev. Clin. Lab. Sci., 25 (1987) 195.
[7] J.M. Candy, A.E. Oakley, J. Klinowski, T.A. Carpenter, R.H. Perry, J.R. Atack, E.K. Perry, G. Blessed, A. Fairbairn and J.A. Edwardson, Lancet, i (1986) 354.
[8] J.P. Landsberg, B. McDonald and F. Watt, Nature (Lond.) (1992) 65.
[9] T.P.A. Kruck, Nature (Lond.), 363 (1993) 119.
[10] Z.S. Khachaturian, Aging, 1 (1989) 17.
[11] D.R. Crapper-McLachlan, Neurobiol. Aging, 7 (1986) 525.
[12] P.O. Ganrot, Envir. Health Perspect., 65 (1986) 363.
[13] H. Meiri, E. Banin, M. Roll and A. Rousseau, Prog. Neurobiol., 40 (1993) 89.
[14] P.F. Good and D.P. Perl, Nature (Lond.), 362 (1993) 418.
[15] A.J. Stern, C. Abraham, P.F. Good, E. Munozgarcia, D.P. Perl and D.P. Selkoe, J. Neuropath. Exp. Neurol., 45 (1986) 361.
[16] J. Díaz-Nido and J. Avila, Neurosci. Lett., 110 (1990) 221.
[17] M. Abdel-Ghany, A.K. El-Sebae and D. Shalloway, J. Biol. Chem., 228 (1993) 11976.
[18] H. Yamamoto, J. Saitoh, S. Yasugawa and E. Miyamoto, J. Neurochem., 55 (1990) 683.

[19] R.A. Nixon, J.F. Clarke, K.B. Logvinenko, M.K.H. Tan, M. Hoult and F. Grynspan, J. Neurochem., 55 (1990) 1950.
[20] T.B. Shea, P. Balikan and M.L. Beerman, FEBS Lett., 307 (1992) 195.
[21] J.F. Leterrier, D. Langui, A. Probst and J. Ulrich, J. Neurochem., 58 (1992) 2060.
[22] R.B. Martin, Clin. Chem., 32 (1986) 1797.
[23] J.D. Birchall, C. Exley, J.S. Chappell and M.J. Phillips, Nature (Lond.) 338, (1989) 146.
[24] E. Epstein, Proc. Natl. Acad. Sci. USA, 91 (1994) 11.
[25] J.A. Edwardson, P.B. Moore, I.N. Ferrier, J.S. Lilley, G.W.A. Newton, J.Berker, J. Templar and J.P. Day, Lancet, 342 (1993) 211.
[26] E.M. Carlisle and M.J. Curran, Alzheimer Dis. Relat. Disorder, 1 (1987) 83.
[27] V.M.-Y. Lee, L. Ötvös, Jr, M.J. Carden, M. Hollosi, B. Diestzschold and R.A. Lazzarini, Proc. Natl. Acad. Sci. USA, 85 (1988) 1998.
[28] V.M.-Y. Lee, L. Ötvös, Jr, M.L. Schmidt and J.Q. Trojanowski, Proc. Natl. Acad. Sci. USA, 85 (1988) 7384.
[29] NO REFERENCE
[30] N. Greenfield and G.D. Fasman, Biochemistry, 8 (1969) 4108.
[31] C.M. Venkatachalam, Biopolymers, 6 (1968) 1425.
[32] L.M. Gierasch, C.M. Deber, V. Madison, C.-H. Niu and E.R. Blout, Biochemistry, 20 (1981) 4730.
[33] F. Bandekar, D.F. Evans, S. Krimm, S.F. Leach, S. Lee, F.R. McQuie, E. Minasian, A. Nemethy, M.S. Pottle, H.A. Scheraga, E.R. Stimson and R.W. Woody, Int. J. Peptide Prot. Res., 19 (1982) 187.
[34] M. Hollósi, M. Kawai and G.D. Fasman, Biopolymers, 24 (1985) 211.
[35] P.Y. Chou and G.D. Fasman, Adv. Enzymol., 47 (1978) 45.
[36] M.W. Meyers, R.A. Lazzarini, V.M.-Y. Lee, W.W. Schlaepfer and D.L. Nelson, EMBO J., 6 (1987) 1617.
[37] NO REFERENCE
[38] F.A. Smith and L.G. Pease, CRC Crit. Rev. Biochem., 8 (1980)315.
[39] A. Perczel, G. Tusnady, M. Hollósi and G.D. Fasman, Prot. Eng., 4 (1991) 669.
[40] A. Perczel, K. Park and G.D. Fasman, Anal. Biochem., 203 (1992) 83.
[41] M. Hollósi, L. Ötvös, Jr., L. Ürge, J. Kajtár, A. Perczel, I. Laczko, Zs. Vadász and G.D. Fasman, Biopolymers, 33 (1993) 497.
[42] M. Hollósi, L. Ürge, A. Perczel, J. Kajtár, I. Teplan, L. Ötvös, Jr. and G.D. Fasman, J. Mol. Biol., 223 (1992) 673.
[43] S. Tokutake, Int. J. Biochem., 22 (1990) 1.
[44] N. Geisler, E. Kaufmann, S. Fischer, U. Plessmann and K. Weber, EMBO J., 2 (1983) 1295.
[45] S.A. Lewis and N.J. Cowan, J. Cell Biol., 100 (1985) 843.
[46] Deleted.
[47] P.A. Robinson, D. Wion and B.H. Anderton, FEBS Lett., 209 (1986) 203.
[48] R.K. Sihag and R.A. Nixon, J. Biol. Chem., 265 (1990) 4166.
[49] M. Hoishi, E. Nishida, Y. Miyata, H. Sakai, T. Miyoshi, H. Ogawara and Y. Akiyama, FEBS Lett., 217 (1987) 237.
[50] J. Baudier and R.O. Cole, J. Biol. Chem., 262 (1987) 17577.
[51] K.S. Kosik, L.D. Orecchio, S. Bakalis, L. Duffy and R.L. Nerve, J. Neurochem. , 51 (1988) 587.
[52] T. Yamauchi and H. Fujisawa, Biochem Biophy. Res. Commun., 109 (1982) 975.
[53] R.D. Sloboda, S.A. Rudolph, J.L. Rosenbaum and P. Greengard, Proc. Natl. Acad. Sci. USA, 72 (1975) 177.
[54] H. Ksiezak-Reding, D.W. Dickson, P. Davies and S.-H. Yen, Proc. Natl. Acad. Sci. USA, 84 (1987) 3410.
[55] N. Nukina, K.S. Kosik and D.J. Selkoe, Proc. Natl. Acad. Sci. USA, 84 (1987) 3415.
[56] V.M.-Y Lee, L. Ötvös, Jr., M.J. Carden, M. Hollósi, B. Dietzschold and R.A. Lazzarini, Proc. Natl. Acad. Sci. USA, 85 (1988) 1998.
[57] V.M.-Y Lee, L. Ötvös, Jr., M.L. Schmidt and J.Q. Trojanowski, Proc. Natl. Acad. Sci. USA, 85 (1988) 7384.
[58] L. Ötvös, M. Hollósi, A. Perczel, B. Dietzschold and G.D. Fasman, J. Protein Chem., 7 (1988) 365.
[59] S. Lefebvre and W.E. Mushyniski, Biochem Biophys. Res. Commun., 145 (1987) 1006.

[60] G.A. Elgavish, D.I. Hay and D.H. Schlesinger, Int. J. Pept. Prot. Res., 23 (1984) 230.
[61] M.S. Mohan and E.H. Abbott, Inorg. Chem., 17 (1978) 2203.
[62] L. Ötvös, I.A. Tangoren, K. Wroblewski, M. Hollosi and V.M.-V. Lee, J. Chromatogr., 512 (1990) 265.
[63] R.W. Woody, in V. Hruby (Ed.), The Peptides 7, Academic Press, New York, 1985, p. 15.
[64] R.W. Woody, in E.R. Bout, F.A. Bovey, M. Goodman and M. Lotan (Eds.), Peptides, Polypeptides and Proteins, J. Wiley, New York, 1974, p. 338.
[65] D.W. Urry, L. Mascotti and J.R. Krivacis, Biochim. Biophys. Acta, 241 (1971) 600.
[66] H.J. Dyson, M. Rance, R.A. Houghton, P.E. Wright and R.A. Lerner, J. Mol. Biol., 201 (1988) 201.
[67] J.R. Parrish and E.R. Blout, Biopolymers, 10 (1971) 1491.
[68] E.W. Ronish and S. Krimm, Biopolymers, 13 (1974) 1635.
[69] V. Sasisekharan, Acta Crystallogr., 12 (1959) 897.
[70] L. Mandelkern, in G.D. Fasman (Ed.), Poly-L-Amino Acids, Marcel Dekker, New York, 1967, p. 675.
[71] I. Glover, I. Haneef, J. Pitts, S. Wood, D. Moss, I. Tickle and T. Blundell, Biopolymers, 22 (1983) 293.
[72] K. Tonan, Y. Dawata and K. Hamaguchi, Biochemistry, 29 (1990) 4424.
[73] A. Bizzi and P. Gambetti, Acta Neuropathol., 71 (1986) 154.
[74] T.B. Shea, J.F. Clarke, T.R. Wheelock, P.A. Paskervich and R.A. Nixon, Brain Res., 492 (1989) 53.
[75] B.E. Tomlinson and J.A. Corsellis, in J.H. Adams, J.A.N. Corsellis and L.W. Ducher (Eds.), Greenfields Neuropathology, Arnold, London, 4th edn., 1984, p.951.
[76] S.A. Lewis, D.Wang and N.J. Cowan, Science, 242 (1988) 936.
[77] N.H. Sternberger, L.A. Sternberger and J. Ulrich, Proc. Natl. Acad. Sci. USA, 82 (1985) 4274.
[78] J.C. Troncoso, J.L. Marsh, M. Häner and U. Aebi, J. Struct. Biol., 103 (1990) 2.
[79] D.P. Perl and W.W. Pendebury, Canad. J. Neurol. Sci., 13 (1986) 441.
[80] M. Hollosi, Z. Shen, A. Perczel and G.D. Fasman, Proc. Natl. Acad. Sci. USA , 91 (1994) 4902.
[81] R.B. Martin, J. Inorg. Chem., 28 (1986) 181.
[82] Z.M. Shen, A. Perczel, M. Hollosi, I. Naypál and G.D. Fasman, Biochemistry , 33 (1994) 9627.
[83] H. Siegal and A. Sigel (Eds.), Metal Ions in Biological Systems, Dekker, New York, 1988, p. 24.
[84] H. van Koningsveld and F.R. Venema, Acta Crystallogr., C47 (1991) 289.
[85] F.H. Allen, J.E. Davies, J.J. Galloy, O. Johnson, O. Kennard, C.F. Macrae, E.M. Mitchel, G.F. Mitchell, J.N. Smith and D.G. Watson, J. Chem. Inf. Comput. Sci., 31 (1991) 187.
[86] F.R. Venema, H. van Koningsveld, J.A. Peters and H. van Bekkum, J. Chem. Soc. Commun. (1990) 699.
[86a] G.G. Bombi, B. Corain and A.A. Sheikh-Osman, Inorg. Chem. Acta, 171 (1990) 79.
[87] T.L. Feng, P.L. Gurian, M.D. Healy and A.R. Baron, Inorg. Chem., 29 (1990) 408.
[88] E.E. Bittar, Z. Xiang and Y.-P. Huang, Biochim. Biophys. Acta, 1108 (1992) 210.
[89] J.W. Nelson and N.R. Kallenbach, Proteins: Struct. Funct. Genet., 1 (1986) 211.
[90] M. Goedert, R.A. Crowther and C.C. Garner, Trends NeuroSci., 14 (1991) 193.
[91] G. Lee, N. Cowan and M. Kirschner, Science, 239 (1988) 285.
[92] F.L. Hall, J.P. Mitchell and P.R. Villiet, J. Biol. Chem., 265 (1990) 6944.
[93] J.P. Landsberg, B. MacDonald and F. Watt, Nature (Lond.), 360 (1992) 65.
[94] P.F. Good, D.P. Perl, L.M. Bierer and J. Schmeidler, Ann. Neurol., 31 (1992) 286.
[95] A.J. Stern, G. Abraham, P.F. Good, E. Mungogracia, E.D.P. Perl and D.J. Selkoe, J. Nueropathol. Exp. Neurol., 45 (1986) 361.
[95a] M. Claudberg and J.G. Joshi, Proc. Natl. Acad. Sci. USA, 90 (1993) 1009.
[96] C. Exley, N.C. Price, S.M. Kelly and J.D. Birchall, FEBS Lett., 324 (1993) 293.
[97] T.E. Lewis (Ed.), Environmental Chemistry and Toxicology of Aluminum, Lewis, Chelsea, MI, 1989.
[98] J.L. Greger, Ciba Found. Symp., 169 (1992) 26.
[99] L. Liss, J. Long and D. Thornton, in T.E. Lewis (Ed.), Environmental Chemistry and Toxicology of Aluminum, Lewis, Chelsea, MI, 1989, 317.
[100] S. Holly, I. Laczo, G.D. Fasman and M. Hollosi, Biochem. Biophys. Res. Commun., 197 (1993) 755.
[101] M. Jackson and H.H. Mantsh, Biochim. Biophys Acta, 1118 (1992) 139.
[102] D.J. Selkoe, R.K.H. Liem, S.H. Sen and M.L. Shelanski, Brain Res., 163 (1979) 235.
[103] G.D. Fasman and C.D. Moore, Proc. Natl. Acad. Sci. USA, 91 (1994) 11232.

[104] C.W. Scott, A. Fieles, L.A. Sygowski and C.B. Caputo, Brain Res., 628 (1993) 77.
[105] D. Langui, B.H. Anderson, J.-P. Brion and J. Ulrich, Brain Res., 438 (1988) 67.
[106] D. Langui, A. Probst, B. Anderton, J.-P. Brion and J. Ulrich, Acta Neuropathol., 80 (1990) 649.
[107] V.M.-Y. Lee, B.J. Balin, L. Ötvös, Jr. and J.Q. Trojanowski, Science, 251 (1991) 675.
[108] C. Exley and J.D. Birchall, Polyhedron, 12 (1993) 1007.
[109] J.D. Brichall, C. Exley, J.S. Chappell and M. Phillips, Nature (Lond.), 338 (1989) 146.
[110] J.D. Brichall and J.C. Chappell, Clin. Chem., 34 (1988) 265.
[111] J.A. Edwardson, P.B. Moore, I.N. Ferrier, J.G. Lilley, G.W.A. Newton, J. Barker, J. Templar and J.P. Day, Lancet, 342 (1993) 211.
[112] L.L. Hench and J. Wilson, Ciba Found. Symp., 121 (1986) 231.
[113] G.D. Fasman, A. Perczel and C.D. Moore, Proc. Natl. Acad. Sci. USA, 92 (1995) 369–371.
[114] G. Perry and M.A. Smith, Clin. Neurosci., 1 (1993) 199.
[115] J. Jarrett and P.T. Landsbury, Jr., Cell, 73 (1993) 1055.
[116] D.J. Selkoe, Annu. Rev. Neurosci., 17 (1994) 489.
[117] G.E. Terzi, G. Hölzemann and J. Seelig, Biochemistry, 33 (1994) 1345.
[118] K. Halverson, P.E. Frasier, D. Kirschner and P.T. Landsberg, Jr., Biochemistry, 29 (1990) 2693.
[119] C.J. Barrow and M.G. Zagorski, Science, 253 (1991) 179.
[120] C.J. Barrow, A. Yasuda, P.T.M. Kenny and M.G. Zagorski, J. Mol. Biol., 225 (1992) 1075.
[121] L.K. Simmons, P.C. May, K.J. Tomaselli, R.E. Rydel, K.S. Fuson, E.F. Brigham, S. Wright, I. Lieberburg, G.W. Becker, D.N. Brems and W.Y. Li, Mol. Pharmacol., 45 (1994) 373.
[122] M. Kawahara, K. Maramoto, K. Kobayashi, H. Mori and Y. Kuroda, Biochem. Biophys. Res. Commun., 198 (1994) 531.
[123] S. Tomski and R.M. Murphy, Arch. Biochem. Biophys., 294 (1992) 630.
[124] L.L. Hench and J. Wilson, in D. Everst and M. O'Conner (Eds.), Silicon Biochemistry, Ciba Foundation 121, Wiley, Chichester, 1986, p. 231.